

## Electronic Supplementary Information (ESI) for:

### Colorimetric “Naked eye” detection of CN<sup>-</sup>, F<sup>-</sup>, CH<sub>3</sub>COO<sup>-</sup> and H<sub>2</sub>PO<sub>4</sub><sup>-</sup> ions by highly nonplanar electron deficient perhaloporphyrins

Nivedita Chaudhri and Muniappan Sankar\*

## Contents

**Fig. S1.** UV-Vis absorption spectra of **1** and **3** and the emission spectra of **1-4** in toluene at 298 K.

**Fig. S2.** <sup>1</sup>H NMR spectra of **1** (top) and **2** (bottom) in CDCl<sub>3</sub> at 298K.

**Fig. S3.** Imino proton region of **1-4** in CDCl<sub>3</sub> at 298K.

**Fig. S4.** Negative ion mode ESI Mass spectrum of H<sub>2</sub>TPPNO<sub>2</sub>Cl<sub>7</sub> (**1**) in CH<sub>3</sub>CN.

**Fig. S5.** The ORTEP diagrams showing top (a) and side (b) views of 2,3,7,8,12,13,17,18-Octachloro-*meso*-tetraphenylporphyrin (**2**).

**Fig. S6.** B3LYP/6-311G (d,p) optimised geometries showing top (a) as well as side (b) views of **1**.

**Fig. S7.** Pictorial representation of frontier orbitals of 2-nitro-3,7,8,12,13,17,18-heptachloro-*meso*-tetraphenylporphyrin (**1**).

**Fig. S8.** CVs and DPVs of **1-4** in CH<sub>2</sub>Cl<sub>2</sub> containing 0.1 M TBAPF<sub>6</sub> at 298 K. Representation of HOMO-LUMO gap of **1-4** obtained from electrochemical studies.

**Fig. S9.** UV-Vis spectral titrations of **2-4** with TFA (protonation studies) in toluene at 298 K.

**Fig. S10.** UV-Vis spectral titrations of **2-4** with TBAOH (deprotonation studies) in toluene at 298 K.

**Fig. S11.** Colorimetric responses of **2-4** while adding of excess of anions in toluene at 298 K.

**Fig. S12.** UV-Vis spectral titrations of **2-4** while increasing [CN<sup>-</sup>] in toluene at 298 K. Insets show the corresponding Hill plots.

**Fig. S13.** UV-Vis spectral titrations of **1-4** while increasing [F<sup>-</sup>] in toluene at 298K. Insets show the corresponding Hill plots.

**Fig. S14.** UV-Vis spectral titrations of **1-4** while increasing [OAc<sup>-</sup>] in toluene at 298K. Insets show the corresponding Hill plots.

**Fig. S15.** UV-Vis spectral titrations of **1-4** while increasing [H<sub>2</sub>PO<sub>4</sub><sup>-</sup>] in toluene at 298K. Insets show the corresponding Hill plots.

**Fig. S16.** Plots of  $\Delta A$  at  $\lambda_{\max}$  vs [CN<sup>-</sup>] or [OAc<sup>-</sup>] or [H<sub>2</sub>PO<sub>4</sub><sup>-</sup>] for **1-4** showing sigmoidal curve indicating the positive cooperative behavior.

**Fig. S17.** Fluorescence spectral titrations (FL quenching) of **1-4** while increasing [F<sup>-</sup>] in toluene at 298 K.

**Fig. S18.** (a) <sup>1</sup>H NMR spectral changes of **1** while [F<sup>-</sup>] in CDCl<sub>3</sub> at 298K. (b) Disappearance of NH protons of **1** upon increasing the aliquots of 0.05 M fluoride ion solution in CDCl<sub>3</sub> at 298K.

**Fig. S19.** DPV traces of **1-4** in absence and presence of excess [F<sup>-</sup>] in CH<sub>2</sub>Cl<sub>2</sub> containing 0.1 M TBAPF<sub>6</sub> at 298K.

**Fig. S20.** DPV titrations of **2-4** while increasing the concentration of F<sup>-</sup> ion in CH<sub>2</sub>Cl<sub>2</sub> containing 0.1 M TBAPF<sub>6</sub> at 298K.

**Fig. S21.** UV-Visible spectral titrations of planar porphyrins (H<sub>2</sub>TPP and H<sub>2</sub>TPP(Ph)<sub>4</sub>) and nonplanar porphyrins (H<sub>2</sub>TPPBr<sub>4</sub> and H<sub>2</sub>TPP(Ph)<sub>8</sub>) while increasing [F<sup>-</sup>] in toluene at 298 K.

**Fig. S22.** Overlayed UV-Visible Spectra of **1-4** with excess of *p*-toluene sulphonic acid, piperidine and fluoride ion in toluene at 298 K.

**Fig. S23.** (a) UV-Vis spectral titrations of **3** with TBACl (0.008 M) in toluene at 298 K. Inset shows the change in Soret region from 460-495 nm; (b) Hill plot log(A<sub>i</sub>-A<sub>0</sub>/A<sub>f</sub>-A<sub>i</sub>) Vs log [Cl<sup>-</sup>] showing 1:1 stoichiometry indicated by slope 1.

**Fig. S24.** (a) Treatment of **1**•2CN<sup>-</sup> complex with aliquots of 1 mM solution TFA at 298 K. (b) Reusability test of regenerated **1** with aliquots of 8 mM solution of CN<sup>-</sup> ions in toluene at 298 K.

**Fig. S25.** (a) Treatment of **2**•2CN<sup>-</sup> complex with sufficient amount of TFA and (b) the colorimetric response for reversibility and reusability test.

**Fig. S26.** (a) Treatment of **3**•2CN<sup>-</sup> complex with sufficient amount of TFA and (b) the colorimetric response for reversibility and reusability test.

**Fig. S27.** (a) Treatment of **4**•2CN<sup>-</sup> complex with sufficient amount of TFA and (b) the colorimetric response for the reversibility and reusability test.

**Table 1.** UV-Vis absorption spectra data of **1** and **3** and fluorescence spectra of **1-4** in toluene at 298 K.

**Table 2.** Crystal structure data of 2,3,7,8,12,13,17,18-Octachloro-*meso*-tetraphenylporphyrin (**2**).

**Table 3.** Selected average bond lengths and bond angles of 2,3,7,8,12,13,17,18-Octachloro-*meso*-tetraphenylporphyrin (**2**).

**Table 4.** Selected average bond lengths and bond angles of 2-nitro-3,7,8,12,13,17,18-heptachloro-*meso*-tetraphenylporphyrin (**1**).

**Table 5.** Electrochemical redox potentials of **1-4** in CH<sub>2</sub>Cl<sub>2</sub> at 298 K.

**Table 6.** Electronic absorption spectral data of **1-4** in presence of excess TFA, TBAOH and various anions in  $\text{CH}_2\text{Cl}_2$  at 298 K.

**Table 7.** The detection limits (LOD) and quantification limits (LOQ) of anions by **1-4** in toluene.

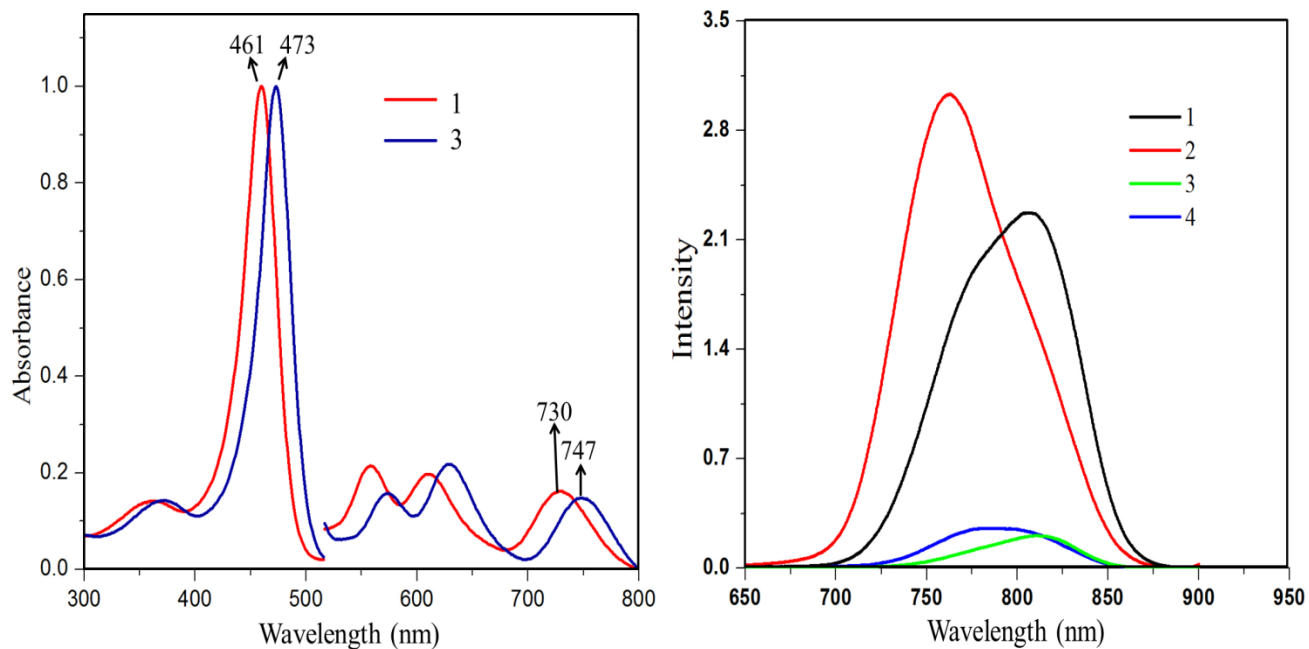


**Figure S1.** UV-Vis absorption spectra of **1** and **3** and fluorescence spectra of **1-4** in toluene at 298 K.

**Table S1.** UV-Visible and fluorescence spectral data of **1-4** in toluene at 298 K.

Porphyrin	B (Bands)	Q (Bands)	$\lambda_{\text{em}}$ , nm
<b>1</b>	363(26.91), 461(190.5)	559(10.23), 612(9.54), 730(7.58)	809
<b>2</b>	356(24.54), 455(204.1)	552(11.48), 601(11.75), 718(6.17)	762
<b>3</b>	371(33.85), 473(239.9)	574(9.55), 628(13.49), 747(9.12)	816
<b>4</b>	364(31.62), 469(257.0)	570(11.48), 623(16.98), 739(8.70)	789

The values in parentheses refer to  $\epsilon \times 10^{-3} \text{ L mol}^{-1} \text{ cm}^{-1}$

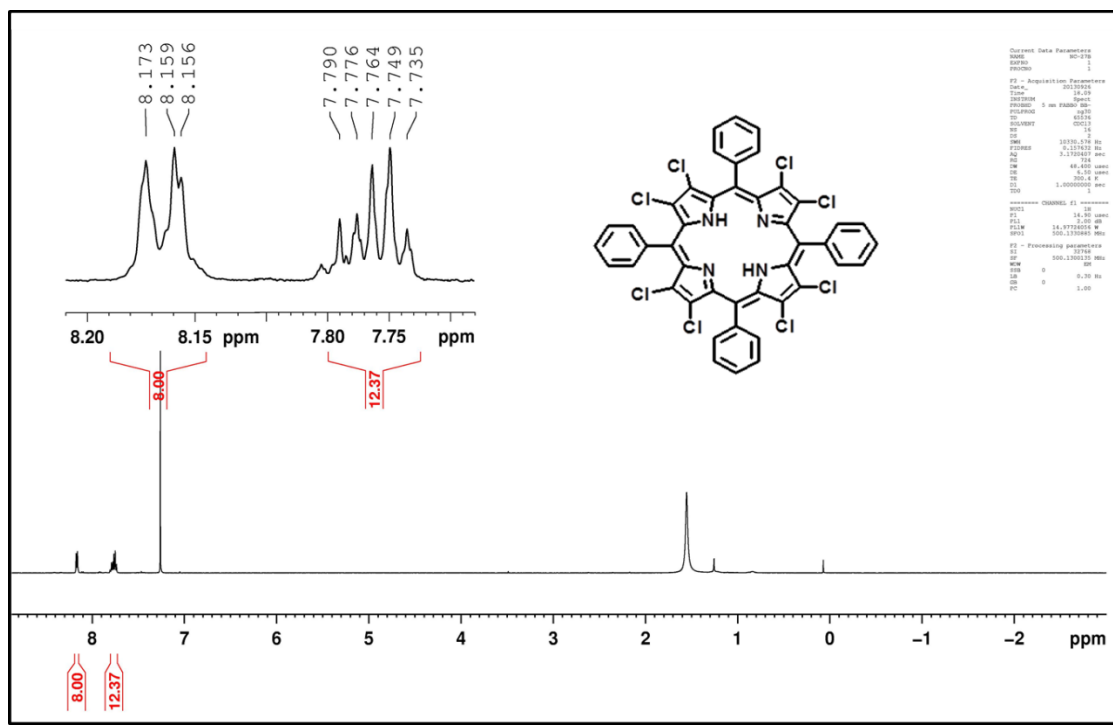
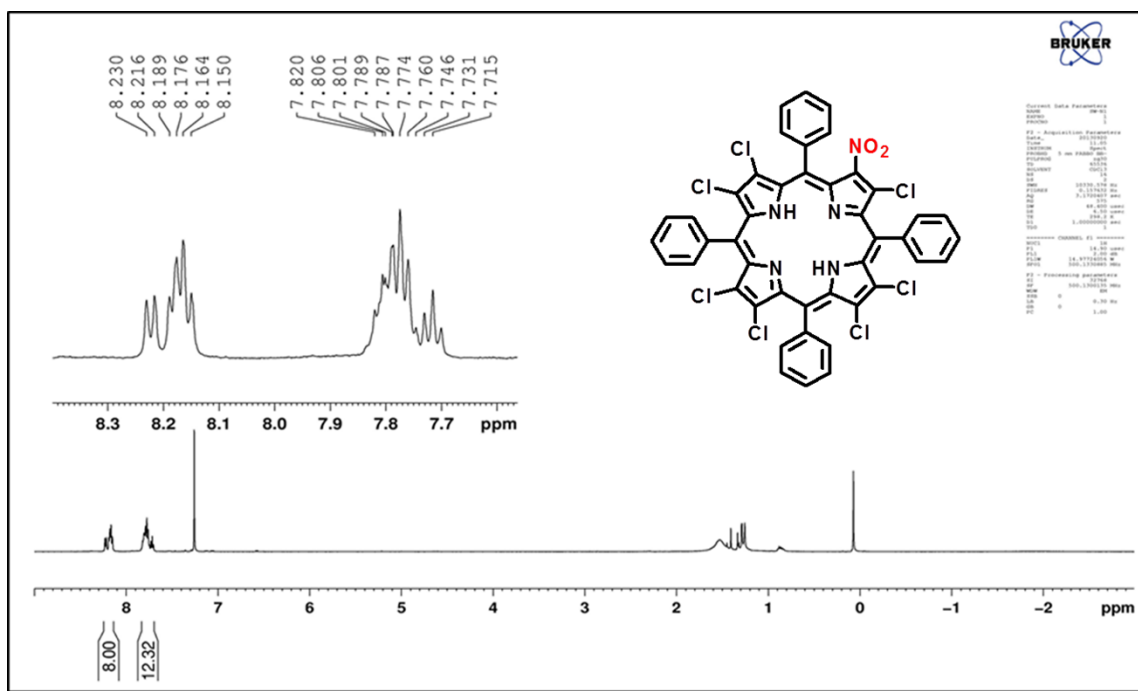


**Figure S2.**  $^1\text{H}$  NMR spectra of **1** (top) and **2** (bottom) in  $\text{CDCl}_3$  at 298K.

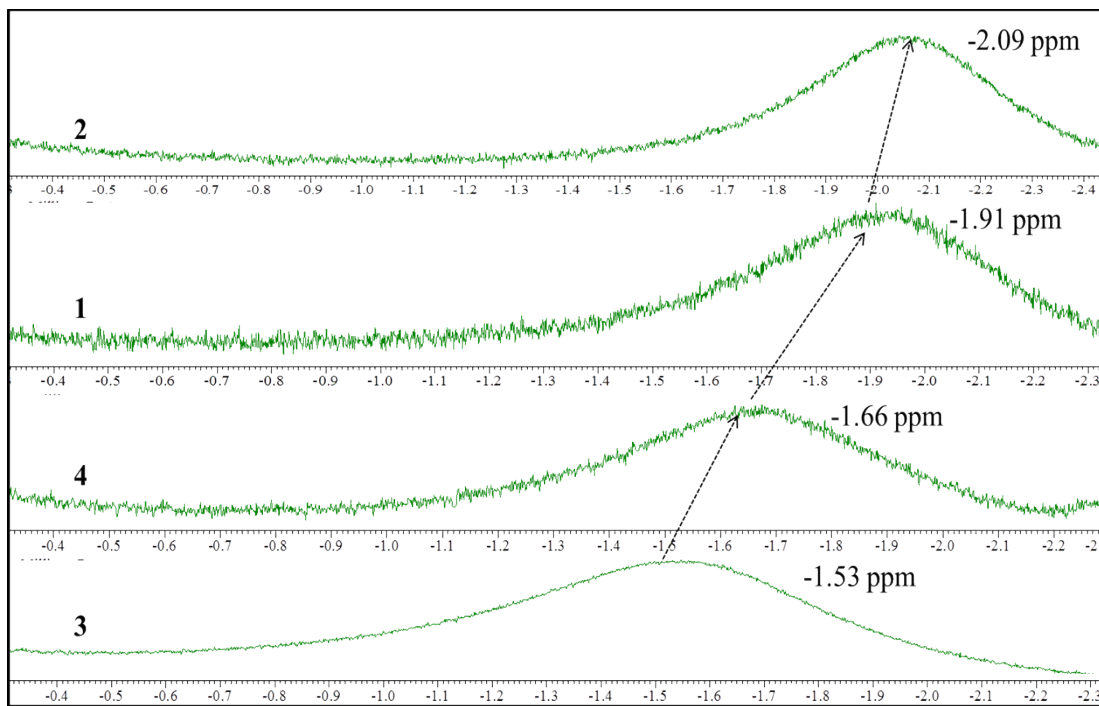


**Figure S3.** Imino protons region of **1-4** in CDCl<sub>3</sub> at 298K

## Display Report

**Analysis Info**

Analysis Name D:\Data\Dr. M. Sankar\NIVIREVIEW.d  
 Method tune\_wide\_Neg.m  
 Sample Name NIVIREVIEW  
 Comment

Acquisition Date 11/18/2014 6:31:55 PM

 Operator IIT ROORKEE  
 Instrument micrOTOF-Q II 10328

**Acquisition Parameter**

Source Type	ESI	Ion Polarity	Negative	Set Nebulizer	0.4 Bar
Focus	Not active	Set Capillary	3000 V	Set Dry Heater	180 °C
Scan Begin	50 m/z	Set End Plate Offset	-500 V	Set Dry Gas	4.0 l/min
Scan End	3000 m/z	Set Collision Cell RF	600.0 Vpp	Set Divert Valve	Source

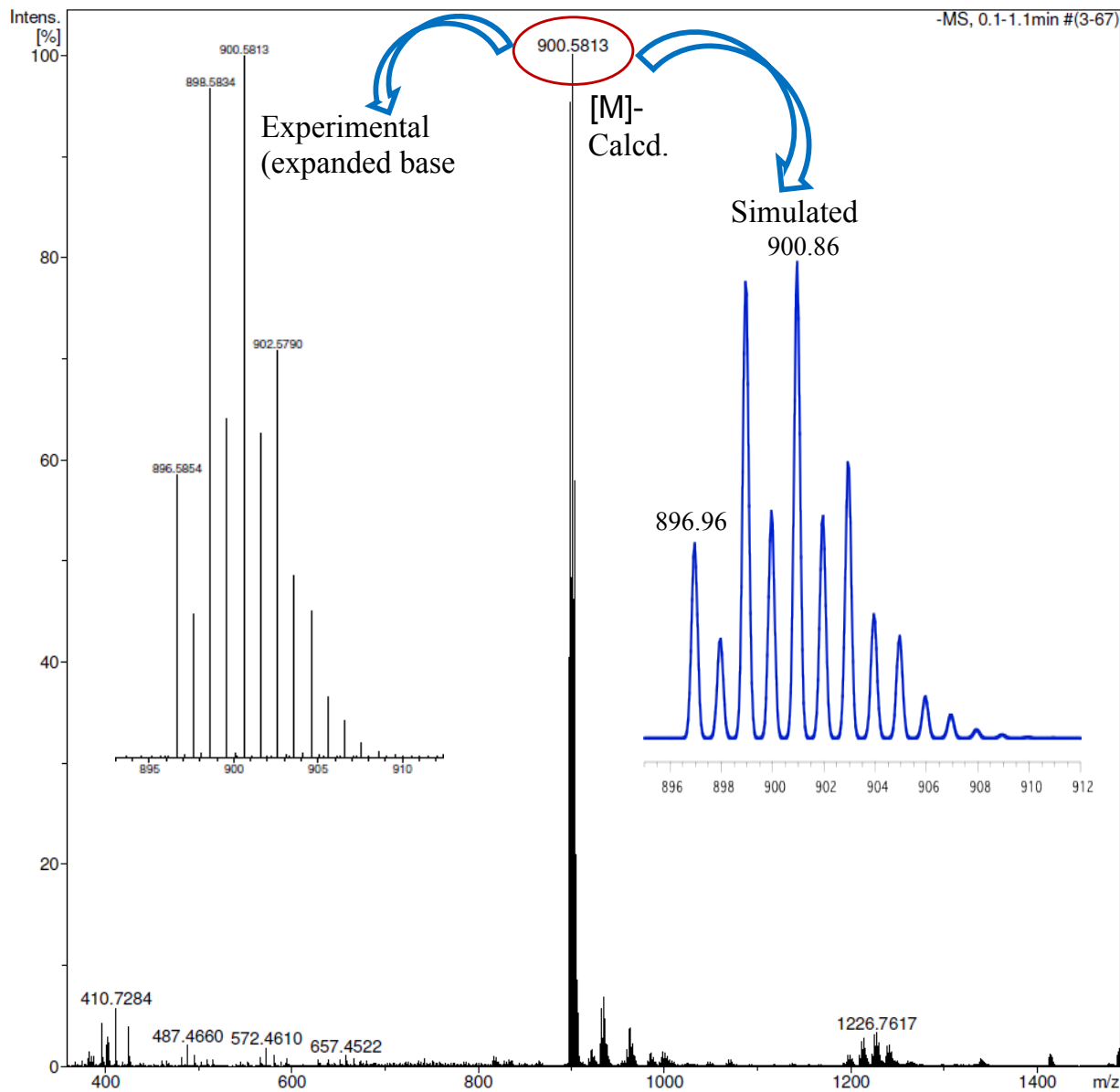


**Figure S4.** Negative ion mode ESI Mass spectrum of  $\text{H}_2\text{TPPNO}_2\text{Cl}_7$  (**1**) in  $\text{CH}_3\text{CN}$ .

**Table S2.** Crystal structure data of 2,3,7,8,12,13,17,18-Octachloro-*meso*-tetraphenylporphyrin (**2**).

	<b>2</b>
Empirical formula	C <sub>48</sub> H <sub>30</sub> N <sub>6</sub> Cl <sub>8</sub> O <sub>2</sub>
Formula wt.	1006.38
Crystal system	Tetragonal
Space group	I 4 <sub>1</sub> /a
a (Å)	19.880(3)
b (Å)	19.880(4)
c (Å)	13.1460(15)
α = β = γ (°)	90
Volume (Å <sup>3</sup> )	5195.5(13)
Z	4
D <sub>cald</sub> (mg/m <sup>3</sup> )	1.287
λ (Å)	0.71073
T (°C)	293 K
No. of total reflns.	1781
No. of indepnt. reflns.	1483
R	0.0113
R <sub>w</sub>	0.3293
CCDC	1033576

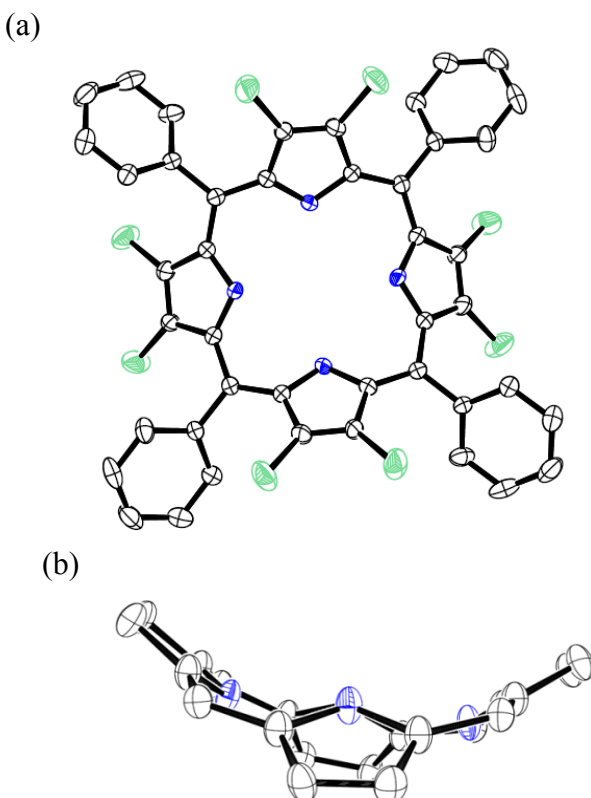


**Figure S5.** The ORTEP diagrams showing top (a) and side (b) views of 2,3,7,8,12,13,17,18-Octachloro-*meso*-tetraphenylporphyrin (**2**).

**Table S3.** Selected average bond lengths and bond angles of 2,3,7,8,12,13,17,18-Octachloro-*meso*-tetraphenylporphyrin (**2**).

Bond length (Å)		Bond angle (°)	
N-H	0.822(8)	N-C <sub>α</sub> -C <sub>m</sub>	123.9(7)
N-C <sub>α</sub>	1.355(10)	N-C <sub>α</sub> -C <sub>β</sub>	107.2(6)
C <sub>α</sub> -C <sub>β</sub>	1.432(10)	C <sub>α</sub> -C <sub>β</sub> -C <sub>β</sub>	107.5(6)
C <sub>β</sub> -C <sub>β</sub>	1.345(11)	C <sub>β</sub> -C <sub>α</sub> -C <sub>m</sub>	128.5(7)
C <sub>α</sub> -C <sub>m</sub>	1.411(10)	C <sub>α</sub> -C <sub>m</sub> -C <sub>α</sub>	120.6(6)
ΔC <sub>β</sub> (Å)	<b>1.2095</b>	C <sub>α</sub> -N-C <sub>α</sub>	110.0(6)
Δ24(Å)	<b>0.5695</b>		

<sup>a</sup>ΔC<sub>β</sub> refers mean plane deviation of β-carbon atoms, <sup>b</sup>Δ24 refers mean plane deviation of 24 core atoms

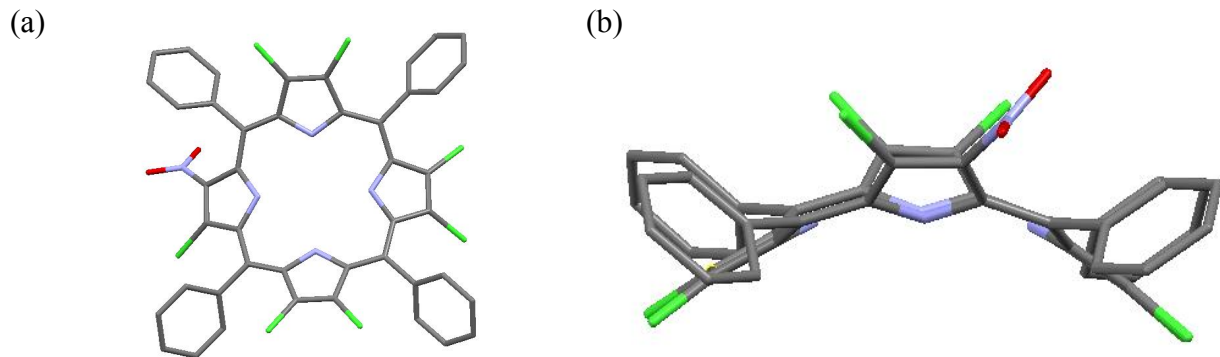
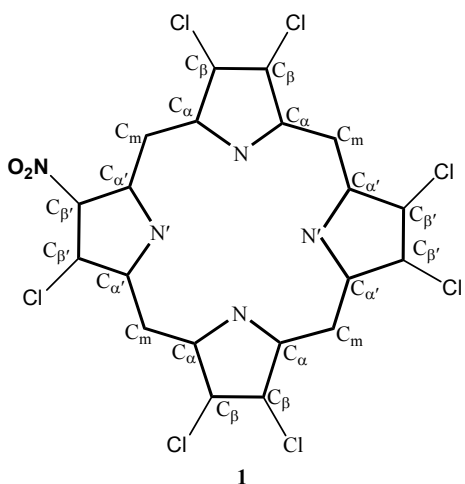


**Figure S6.** B3LYP/6-311G(d,p) optimised geometries showing top (a) as well as side (b) views of **1**.

**Table S4.** Selected average bond lengths and bond angles of 2-nitro-3,7,8,12,13,17,18-heptachloro-*meso*-tetraphenylporphyrin (**1**).



Bond length (Å)		Bond angle (°)	
N'- H	1.011	N- C <sub>α</sub> -C <sub>m</sub>	124.025
N-C <sub>α</sub>	1.360	N-C <sub>α'</sub> -C <sub>m</sub>	124.623
N'-C <sub>α'</sub>	1.374	N-C <sub>α</sub> -C <sub>β</sub>	109.335
C <sub>α</sub> -C <sub>β</sub>	1.462	N-C <sub>α'</sub> -C <sub>β'</sub>	105.068
C <sub>α'</sub> -C <sub>β</sub> '	1.440	C <sub>β</sub> -C <sub>α</sub> -C <sub>m</sub>	126.323
C <sub>β</sub> -C <sub>β</sub> '	1.360	C <sub>β'</sub> -C <sub>α'</sub> -C <sub>m</sub>	130.183
C <sub>β</sub> '-C <sub>β</sub> '	1.376	C <sub>α</sub> -C <sub>m</sub> -C <sub>α'</sub>	122.755
C <sub>α</sub> -C <sub>m</sub>	1.416	C <sub>α</sub> -C <sub>β</sub> -C <sub>β</sub> '	106.635
C <sub>α'</sub> -C <sub>m</sub>	1.407	C <sub>α</sub> -C <sub>β'</sub> -C <sub>β</sub> '	108.440
$\Delta C_{\beta}(\text{\AA})^a$	<b>1.212</b>	C <sub>α</sub> -N-C <sub>α</sub>	107.725
$\Delta 24(\text{\AA})^b$	<b>0.515</b>	C <sub>α'</sub> -N-C <sub>α'</sub>	112.685

<sup>a</sup> $\Delta C_{\beta}$  refers mean plane deviation of  $\beta$ -carbon atoms, <sup>b</sup> $\Delta 24$  refers mean plane deviation of 24 core atoms.

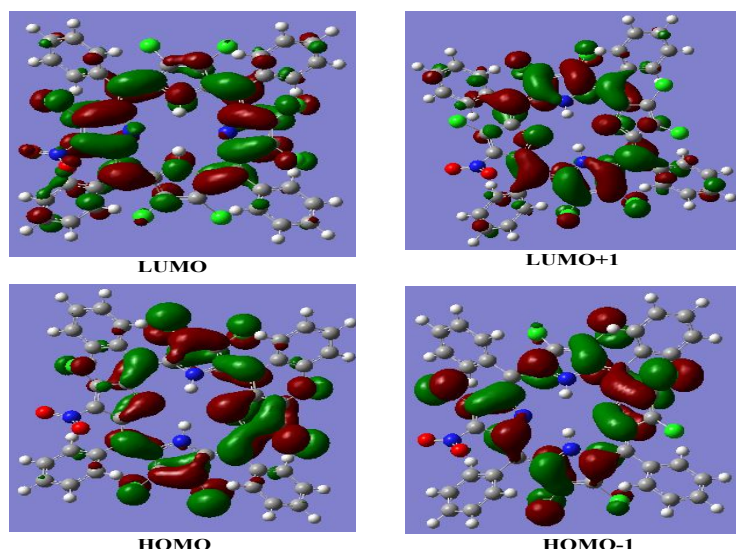


**Figure S7.** Pictorial representation of frontier orbitals of 2-nitro-3,7,8,12,13,17,18-heptachloro-*meso*-tetraphenylporphyrin (**1**).

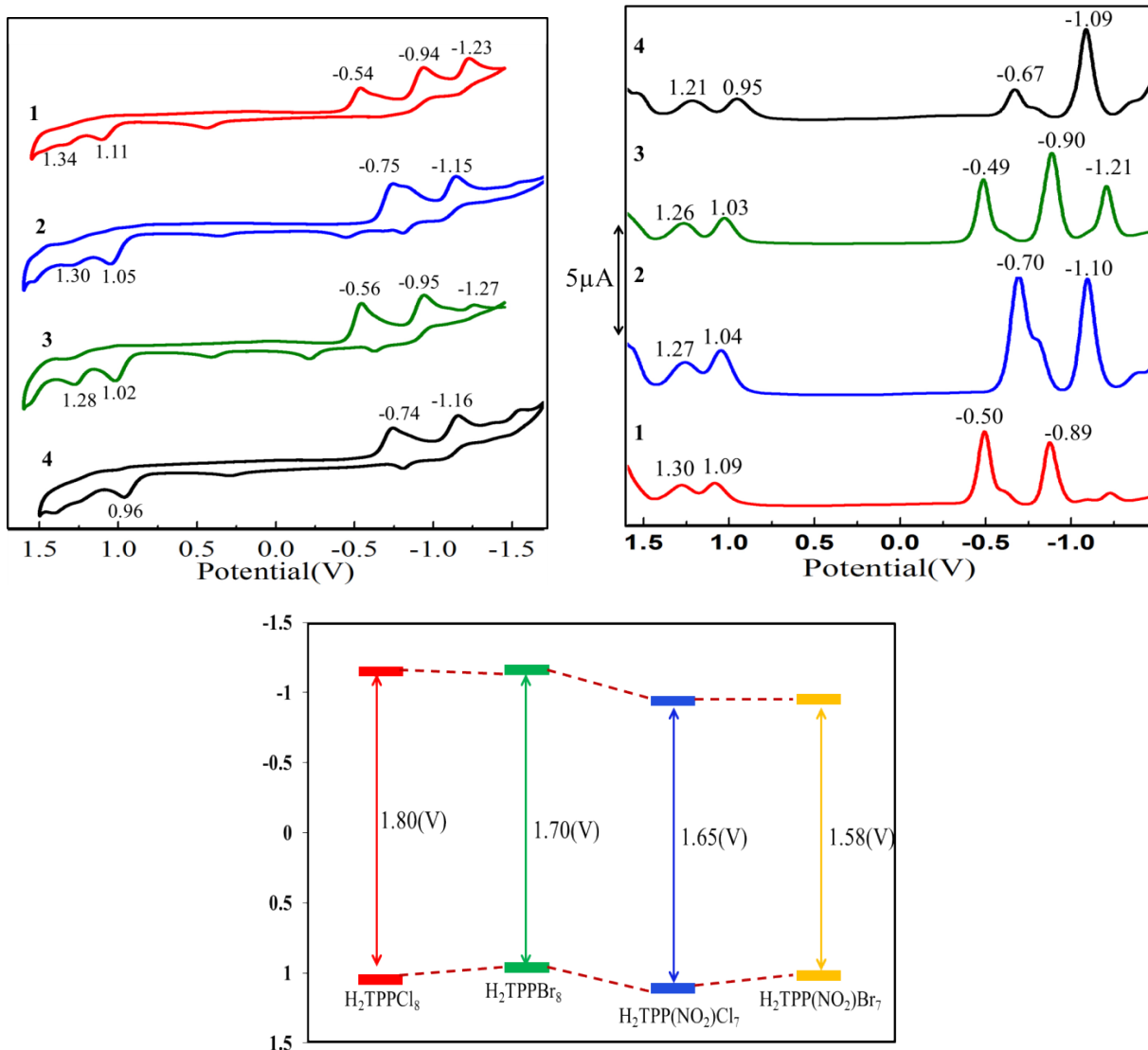


**Figure S8.** CVs and DPVs of **1-4** in  $\text{CH}_2\text{Cl}_2$  containing 0.1 M TBAPF<sub>6</sub> at 298 K (top). Representation of HOMO-LUMO gap of **1-4** obtained from electrochemical studies (bottom).

**Table S5.** Electrochemical redox potentials<sup>a</sup> of **1-4** in  $\text{CH}_2\text{Cl}_2$  at 298K.

Porphyrin	Oxidation (Volts)			Reduction(Volts)			$\Delta E_{1/2} (\text{I}_{\text{ox}}-\text{I}_{\text{red}})$ (Volts)
	I	II	I	II	III		
<b>1</b>	1.11	1.34	-0.54	-0.94	-1.23		1.65
<b>2</b>	1.05	1.30	-0.75	-1.15	-		1.80
<b>3</b>	1.02	1.28	-0.56	-0.95	-1.27		1.58
<b>4</b>	0.96	1.21*	-0.74	-1.16	-		1.70

<sup>a</sup>vs Ag/AgCl, \*data obtained from DPV, all are irreversible potentials.

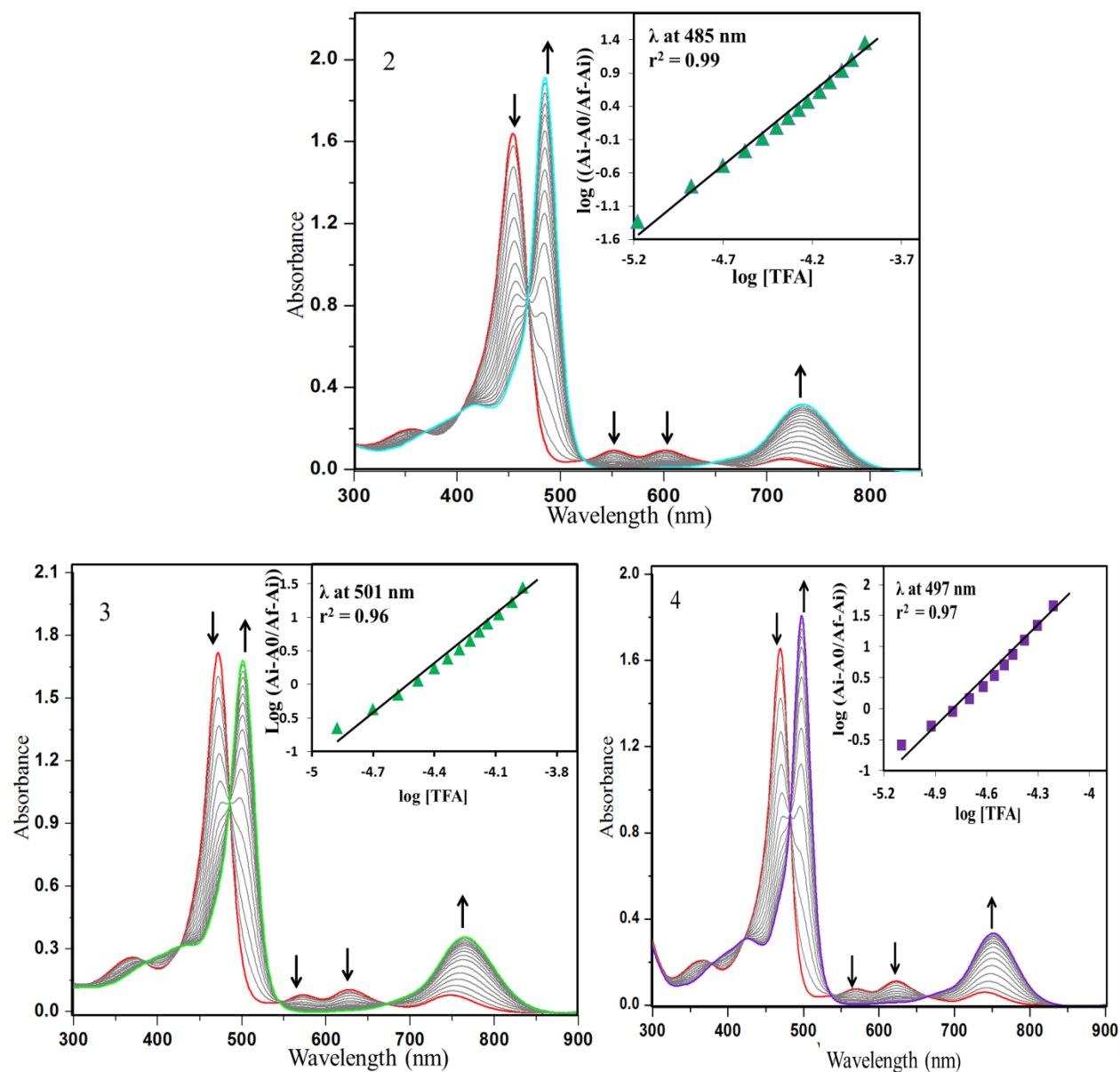


**Figure S9.** UV-Vis spectral titrations of **2-4** with TFA (protonation studies) in toluene at 298 K.

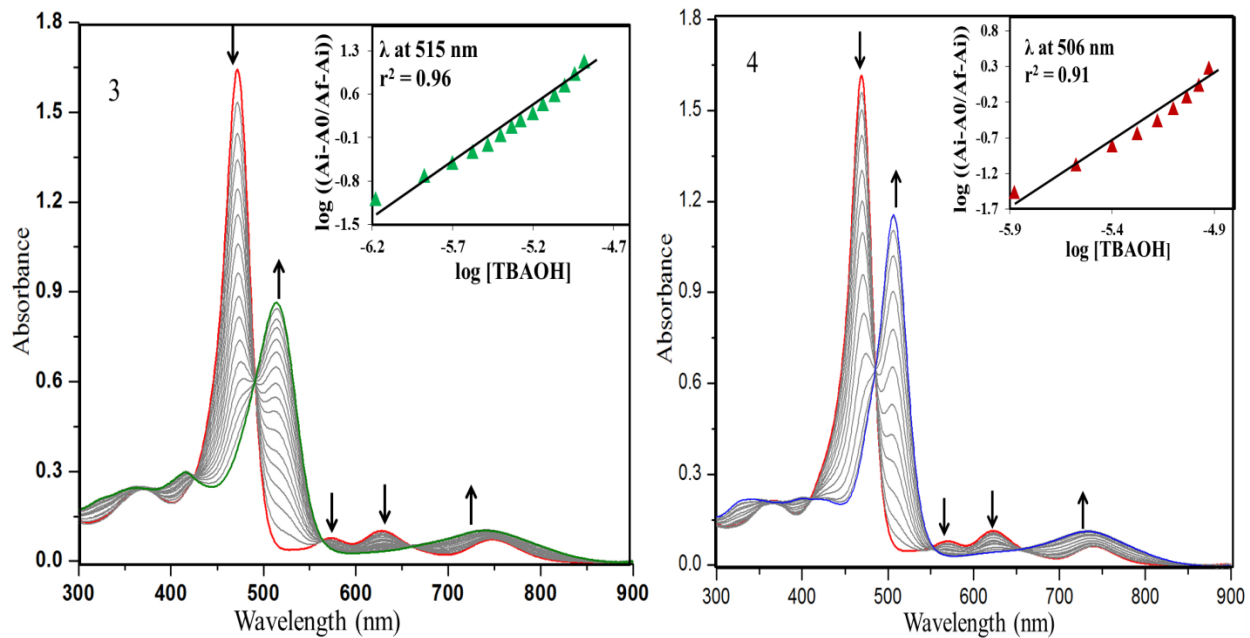
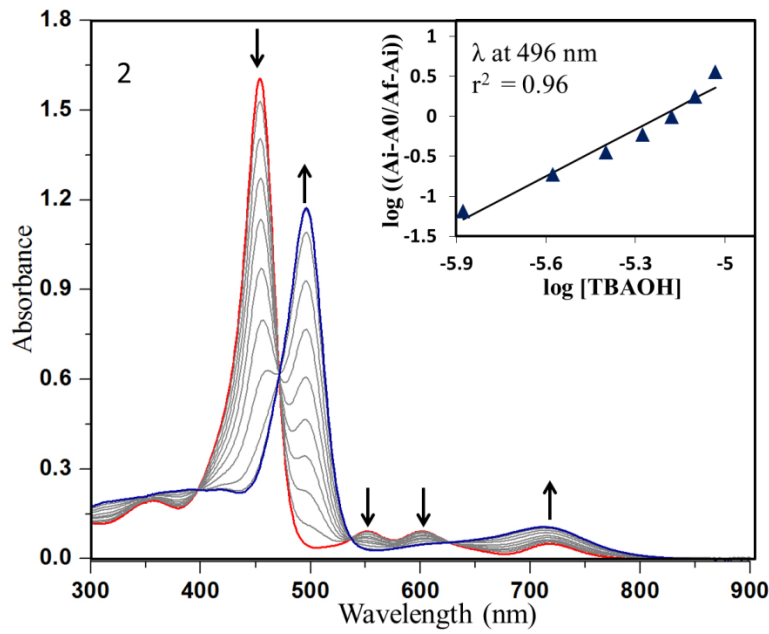


**Figure S10.** UV-Vis spectral titrations of **2-4** with TBAOH (deprotonation studies) in toluene at 298 K.

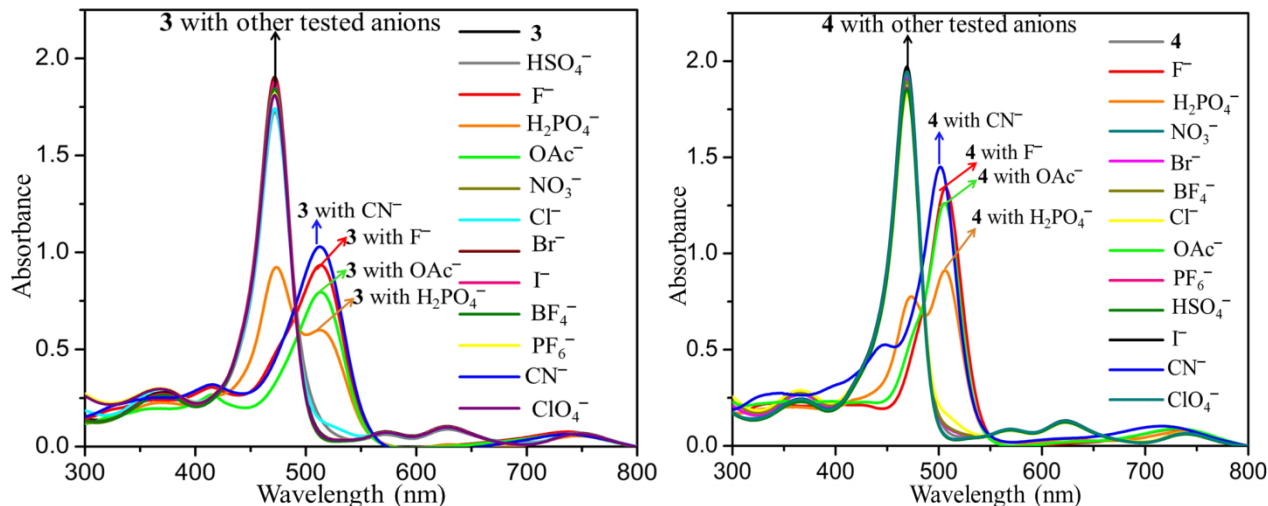
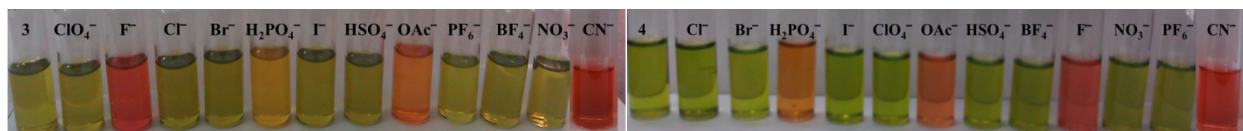
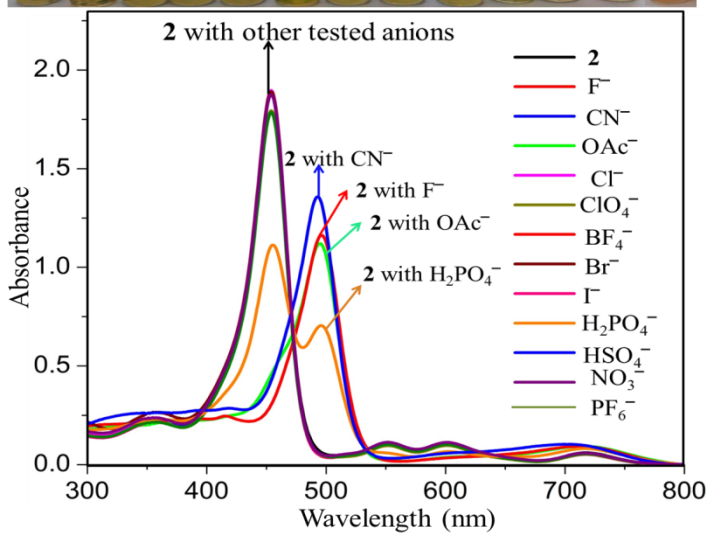


**Figure S11.** Colorimetric responses of **2-4** while adding of excess of anions in toluene at 298 K.

**Table S6.** Electronic absorption spectral data of **1-4** in presence of excess TFA, TBAOH and various anions in  $\text{CH}_2\text{Cl}_2$  at 298K.

Porphyrin	B band(s)	Q band
[1•2H] <sup>2+</sup>	491 (94.16)	754 (11.95)
[2•2H] <sup>2+</sup>	415(22.14), 483 (151.99)	734 (24.90)
[3•2H] <sup>2+</sup>	501 (93.75)	768 (7.99)
[4•2H] <sup>2+</sup>	425(18.95), 495 (149.03)	750 (22.03)
<b>Deprotonation</b>		
[1-2H] <sup>2-</sup>	409(17.69), 506 (47.81)	726 (4.01)
[2-2H] <sup>2-</sup>	492 (87.13)	713(7.25)
[3-2H] <sup>2-</sup>	414(15.94), 516 (50.21)	743(2.92)
[4-2H] <sup>2-</sup>	401(15.55), 505 (88.66)	735 (6.11)
<b>Cyanide</b>		
[1+2CN <sup>-</sup> ]	412(19.24), 506 (52.04)	720 (4.26)
[2+2CN <sup>-</sup> ]	414(22.17), 492 (109.75)	713 (8.84)
[3+2CN <sup>-</sup> ]	414(17.19), 514 (53.06)	740 (3.41)
[4+2CN <sup>-</sup> ]	444(31.98), 503 (94.52)	723 (6.79)
<b>Fluoride</b>		
[1+2F <sup>-</sup> ]	490(20.57), 506 (55.65)	721 (4.91)
[2+2F <sup>-</sup> ]	492 (104.11)	710 (8.59)
[3+2F <sup>-</sup> ]	414(1.35), 516 (56.87)	739 (3.75)
[4+2F <sup>-</sup> ]	398(17.56), 504 (98.41)	731 (7.34)
<b>Acetate</b>		
[1+2CH <sub>3</sub> COO <sup>-</sup> ]	410(22.07), 506 (58.50)	719 (5.22)
[2+2CH <sub>3</sub> COO <sup>-</sup> ]	492 (77.95)	714 (7.04)
[3+2CH <sub>3</sub> COO <sup>-</sup> ]	414(18.35), 516 (59.79)	737 (3.90)
[4+2CH <sub>3</sub> COO <sup>-</sup> ]	472(53.79), 504 (88.60)	734 (6.76)
<b>Dihydrogenphosphate</b>		
[1+2H <sub>2</sub> PO <sub>4</sub> <sup>-</sup> ]	411(22.98), 506 (59.51)	721 (5.38)
[2+2H <sub>2</sub> PO <sub>4</sub> <sup>-</sup> ]	358(19.97), 456(73.95),492 (80.46)	716 (8.01)
[3+2H <sub>2</sub> PO <sub>4</sub> <sup>-</sup> ]	416(19.93), 516 (60.79)	741 (4.03)
[4+2H <sub>2</sub> PO <sub>4</sub> <sup>-</sup> ]	471(57.90), 504 (90.30)	734 (7.22)

Values in parentheses represent  $\varepsilon \times 10^{-3} \text{ L mol}^{-1} \text{ cm}^{-1}$

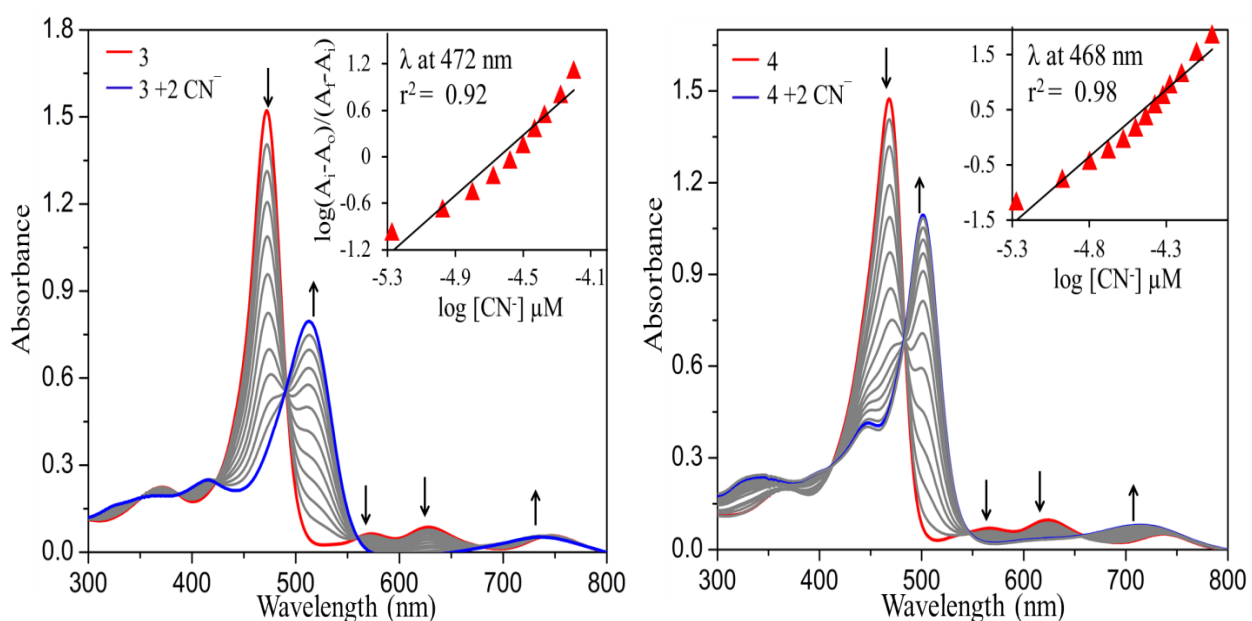
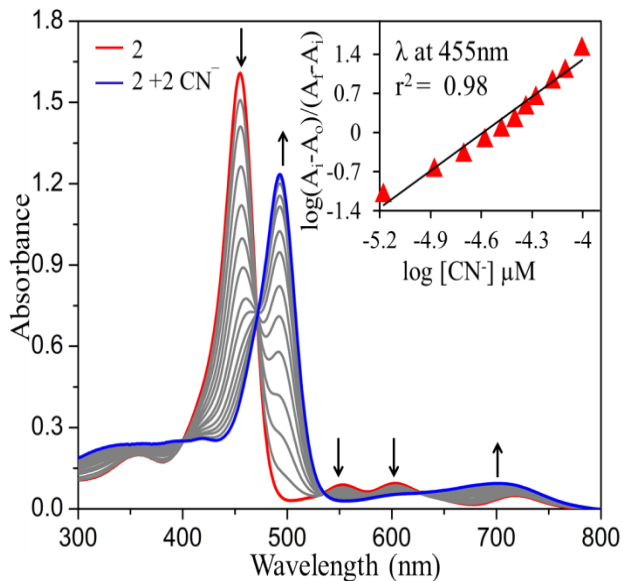


**Figure S12.** UV-Vis spectral titrations of **2-4** while increasing  $[\text{CN}^-]$  in toluene at 298K. Insets show the corresponding Hill plots.

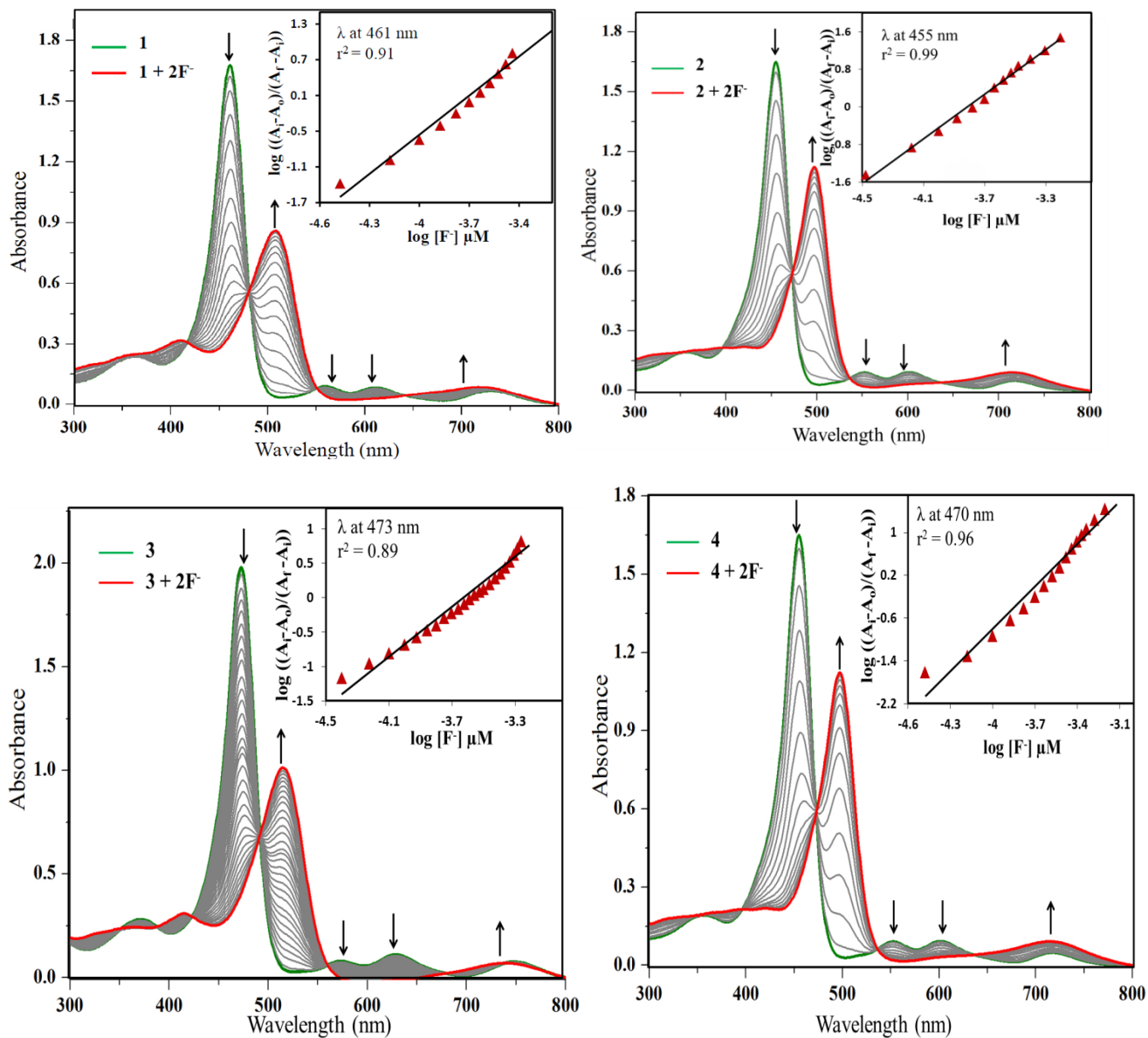


**Figure S13.** UV-Vis spectral titrations of **1-4** while increasing  $[F^-]$  in toluene at 298K. Insets show the corresponding Hill plots.

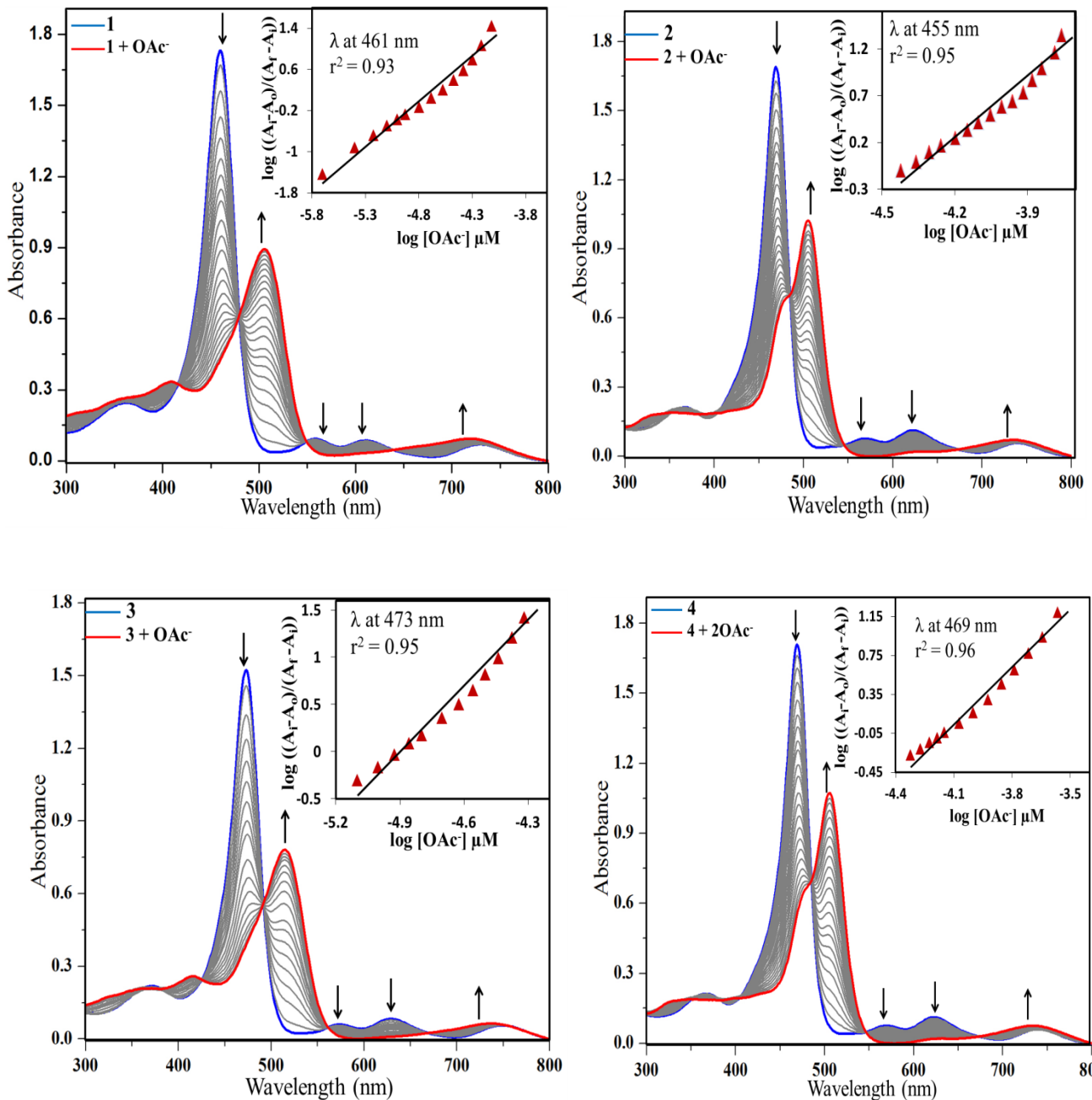


**Figure S14.** UV-Vis spectral titrations of **1-4** while increasing [OAc<sup>-</sup>] in toluene at 298K. Insets show the corresponding Hill plots.

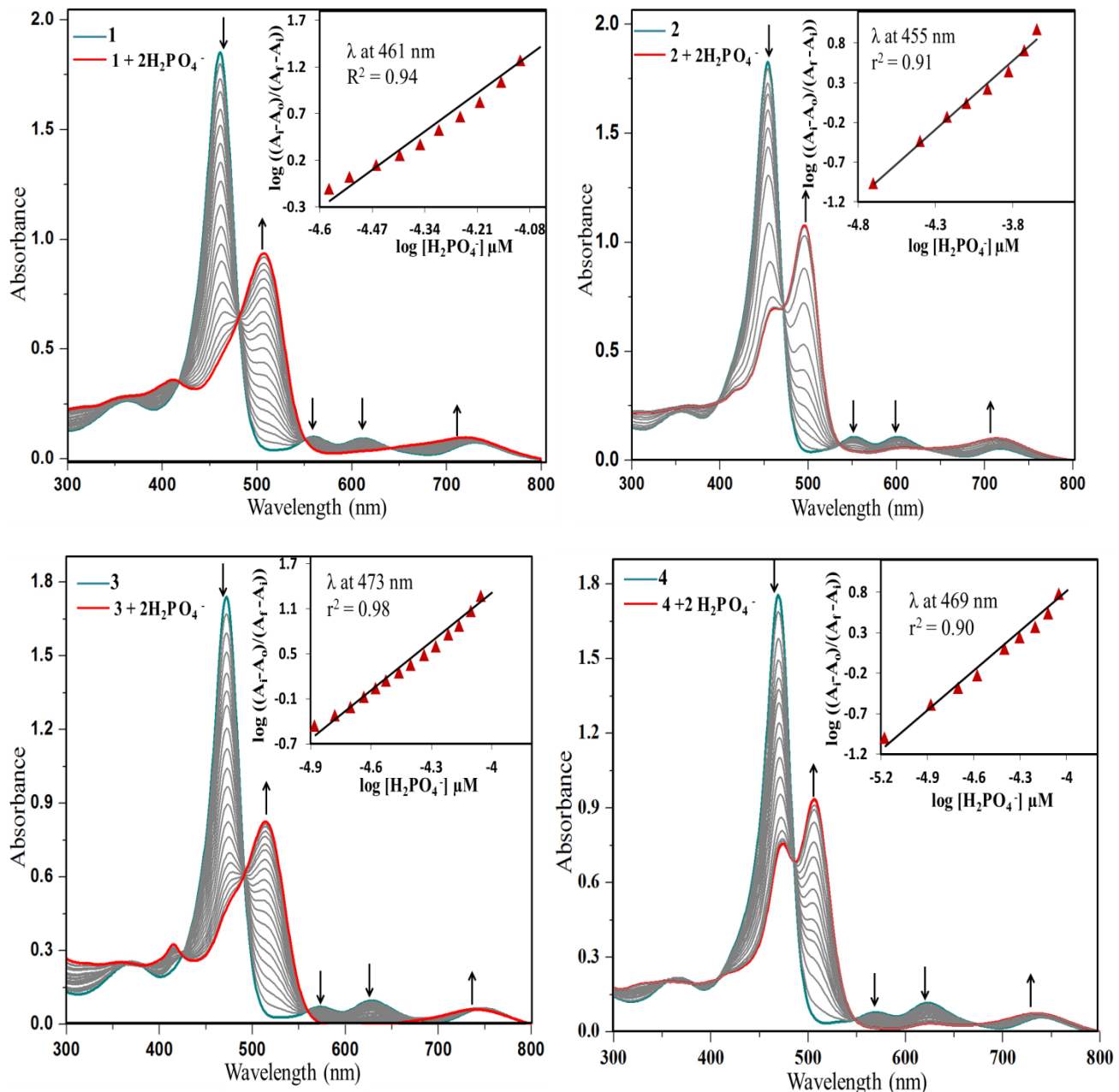


**Figure S15.** UV-Vis spectral titrations of **1-4** while increasing [H<sub>2</sub>PO<sub>4</sub><sup>-</sup>] in toluene at 298K. Insets show the corresponding Hill plots.

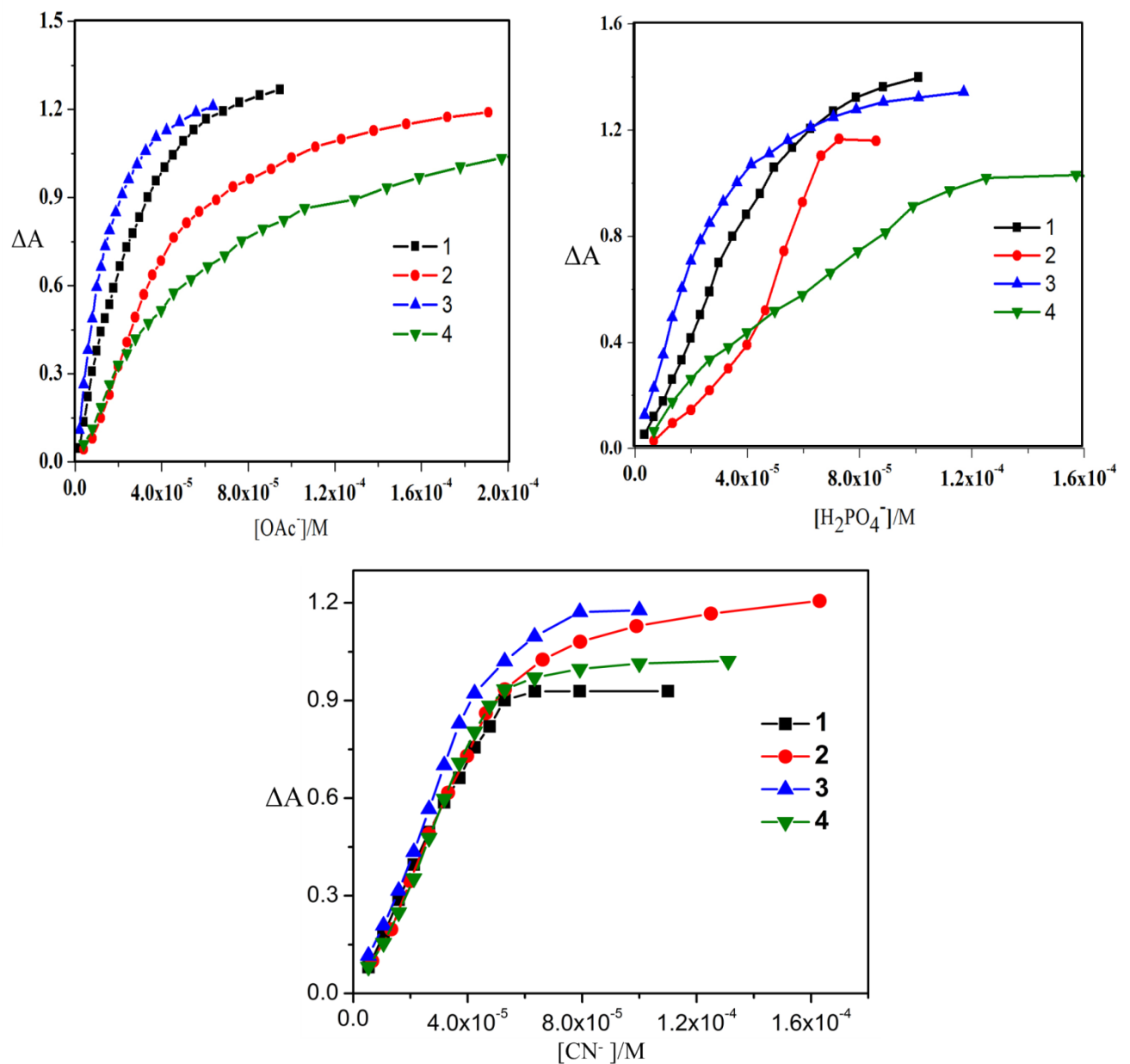


**Figure S16.** Plots of  $\Delta A$  at  $\lambda_{\max}$  vs  $[OAc^-]$  or  $[H_2PO_4^-]$  or  $[CN^-]$  for **1-4** showing sigmoidal curve indicating the positive cooperative behavior.

**Table S7.** The detection limits (LOD) and quantification limits (LOQ) of anions by **1-4** in toluene at 298K.

Por	CN <sup>-</sup>		F <sup>-</sup>		CH <sub>3</sub> COO <sup>-</sup>		H <sub>2</sub> PO <sub>4</sub> <sup>-</sup>	
	LOD	LOQ	nM	LOD	LOQ	nM	LOD	LOQ
	nM (ppb)	(ppb)	nM (ppb)	nM (ppb)	nM (ppb)	ppb)	nM (ppb)	nM (ppb)
<b>1</b>	7.3(0.19)	22.3(0.87)	6.0(0.11)	18.2(0.34)	8.2(0.48)	24.7(1.45)	7.7(0.75)	23.4(2.26)
<b>2</b>	9.5(0.24)	28.7(0.75)	8.4(0.16)	25.4(0.48)	9.7(0.57)	29.4(1.73)	9.6(0.93)	29.2(2.83)
<b>3</b>	8.6(0.22)	26.1(0.68)	7.4(0.14)	22.3(0.42)	10.0(0.59)	30.3(1.78)	10.3(1.00)	31.3(3.04)
<b>4</b>	8.3(0.21)	25.3(0.66)	8.4(0.16)	25.3(0.48)	8.7(0.51)	26.2(1.55)	8.6(0.83)	26.0(2.52)

nM and ppb represent nanomolar and parts per billion respectively

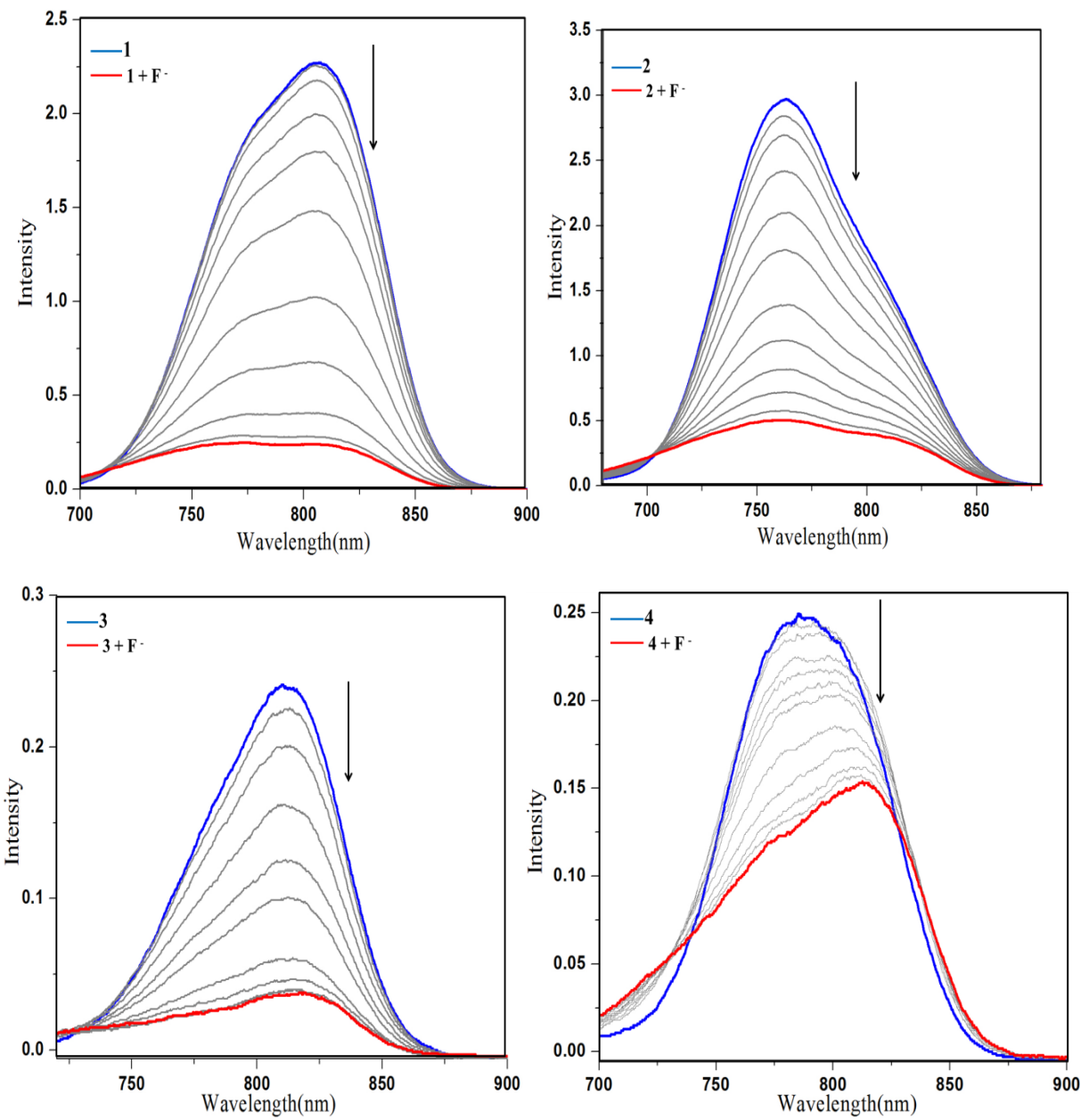
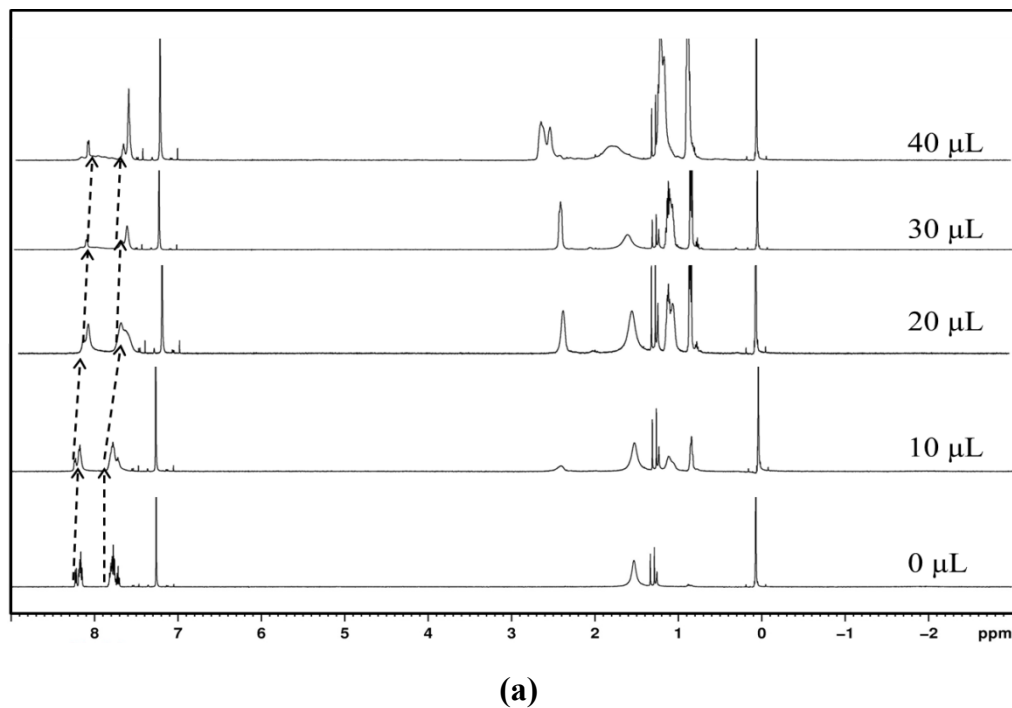
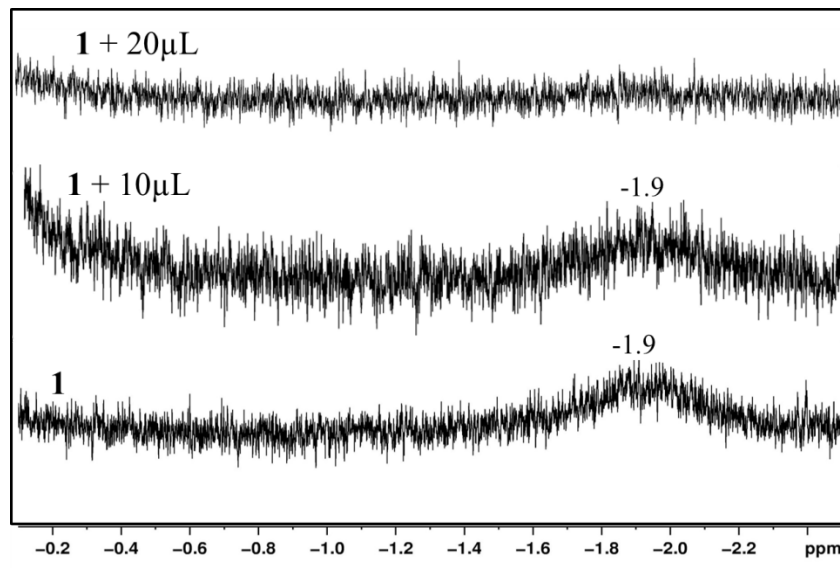


**Figure S17.** Fluorescence spectral titrations (FL quenching) of **1-4** while increasing  $[\text{F}^-]$  in toluene at 298K.



(a)



(b)

**Figure 18.** (a) <sup>1</sup>H NMR spectral changes of **1** while  $[\text{F}^-]$  in  $\text{CDCl}_3$  at 298K. (b) Disappearance of NH protons of **1** upon increasing the aliquots of 0.05 M fluoride ion solution in  $\text{CDCl}_3$  at 298K.

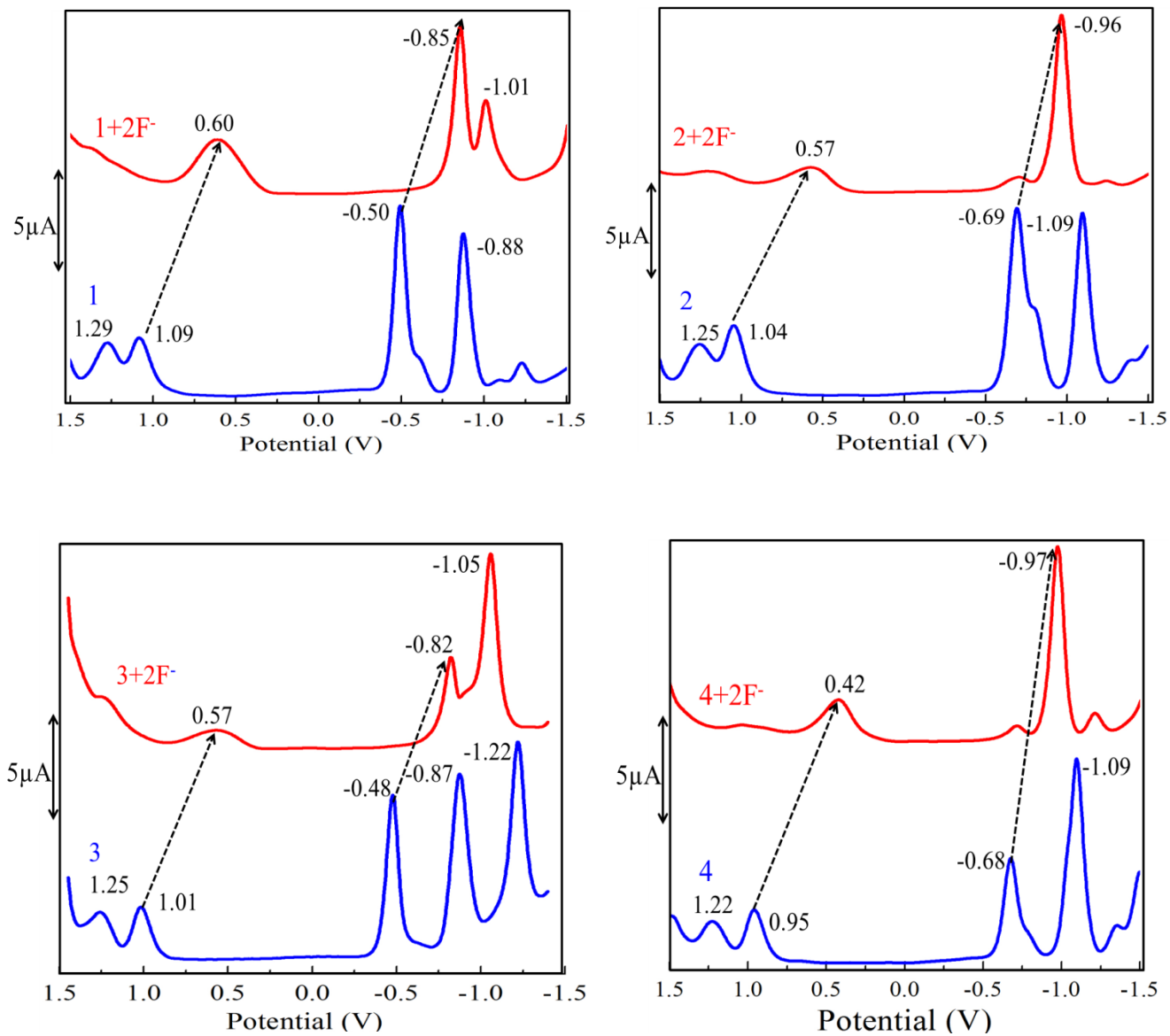


**Figure S19.** DPV traces of **1-4** in absence and presence of excess [F<sup>-</sup>] in  $\text{CH}_2\text{Cl}_2$  containing 0.1 M TBAPF<sub>6</sub> at 298K.

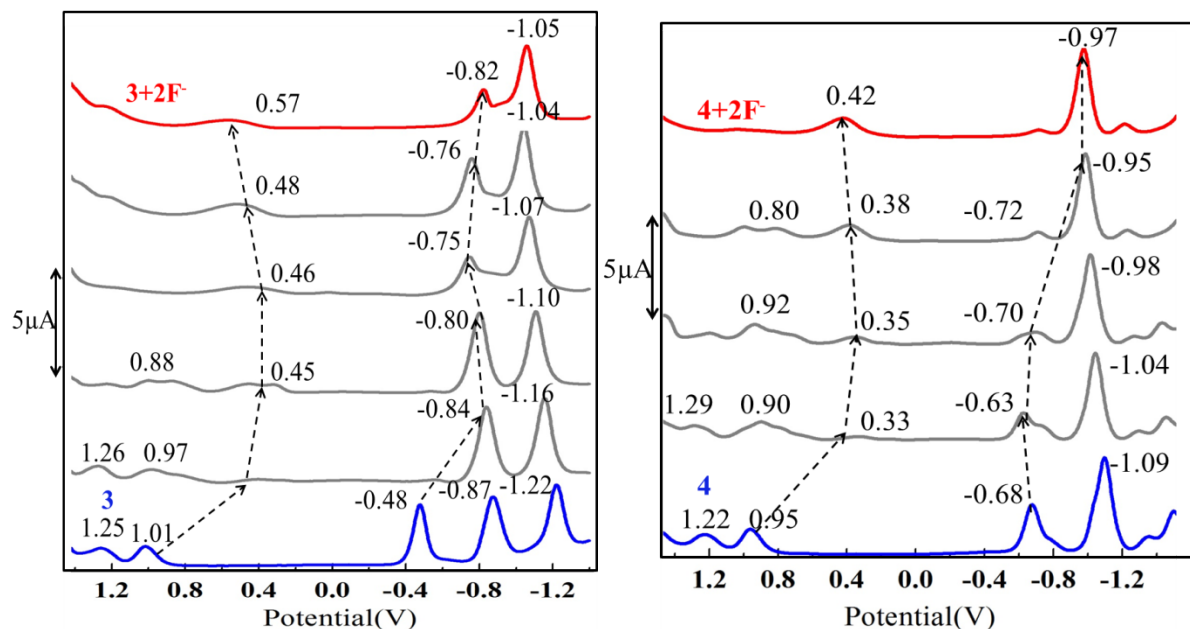
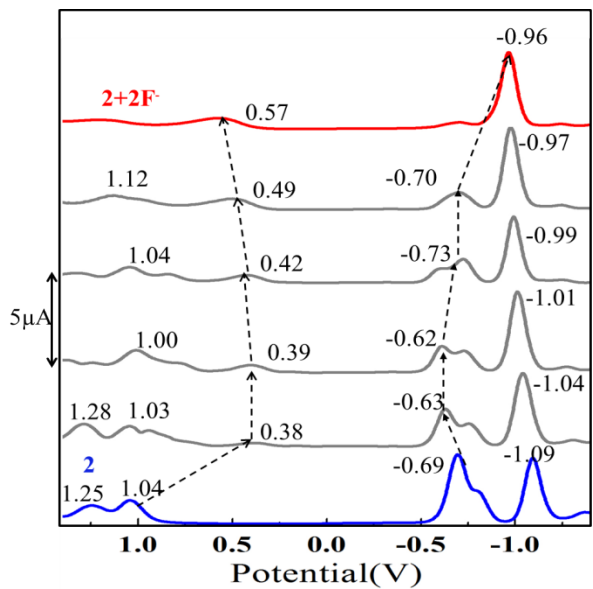


**Figure S20.** DPV titrations of **2-4** while increasing the concentration of F<sup>-</sup> ion in  $\text{CH}_2\text{Cl}_2$  containing 0.1 M TBAPF<sub>6</sub> at 298K.

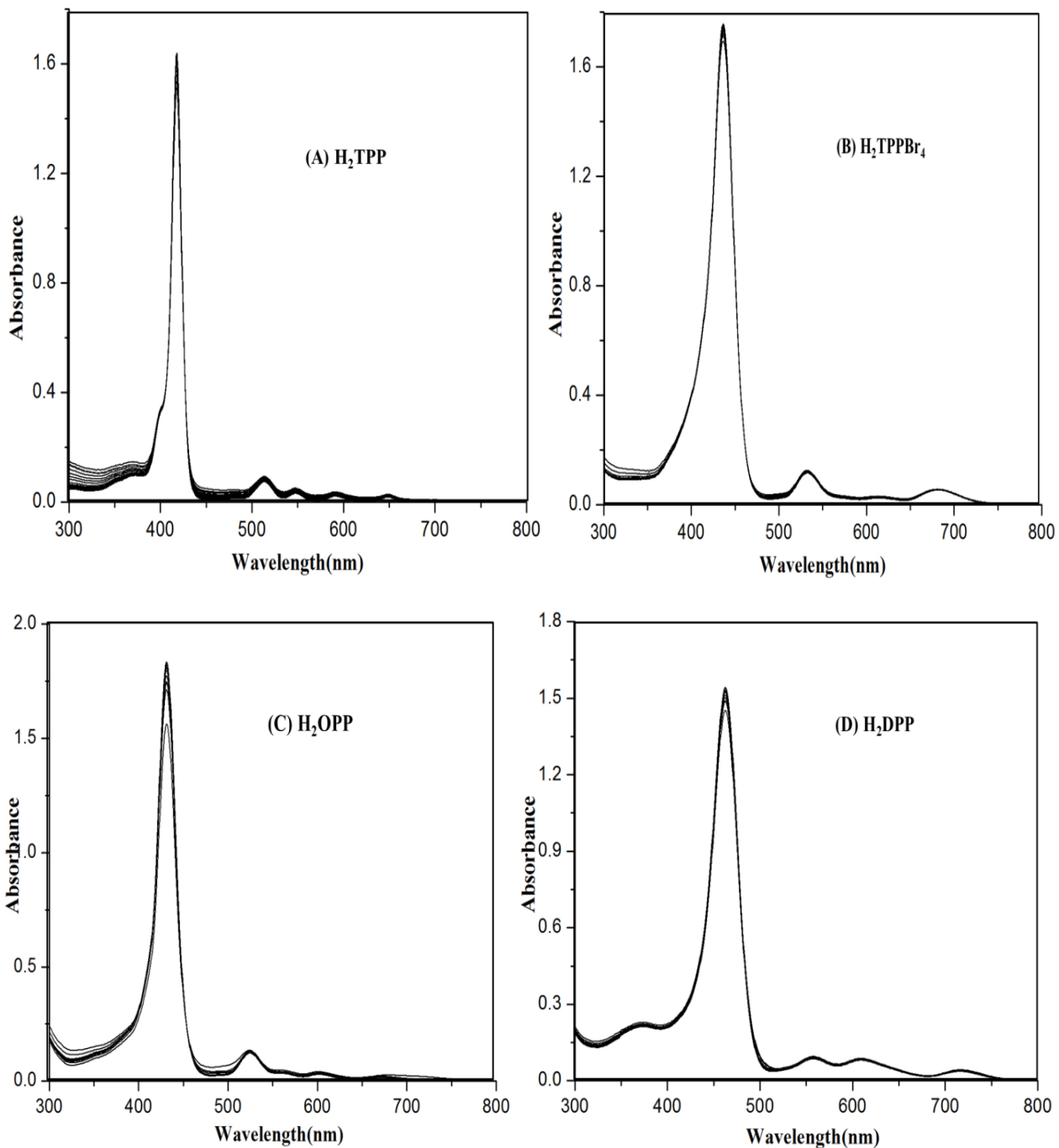


**Figure S21:** UV-Visible spectral titrations of planar porphyrins (*meso*-tetraphenylporphyrin ( $\text{H}_2\text{TPP}$ ) and 2,3,5,10,15,17,18,20-octaphenylporphyrin ( $\text{H}_2\text{TPP}(\text{Ph})_4$ ) and nonplanar porphyrins (2,3,12,13-tetrabromo-*meso*-tetraphenylporphyrin ( $\text{H}_2\text{TPPBr}_4$ ) and 2,3,5,7,8,10,12,13,15,17,18,20-dodecaphenylporphyrin ( $\text{H}_2\text{TPP}(\text{Ph})_8$ )) while increasing  $[\text{F}^-]$  in toluene at 298 K.

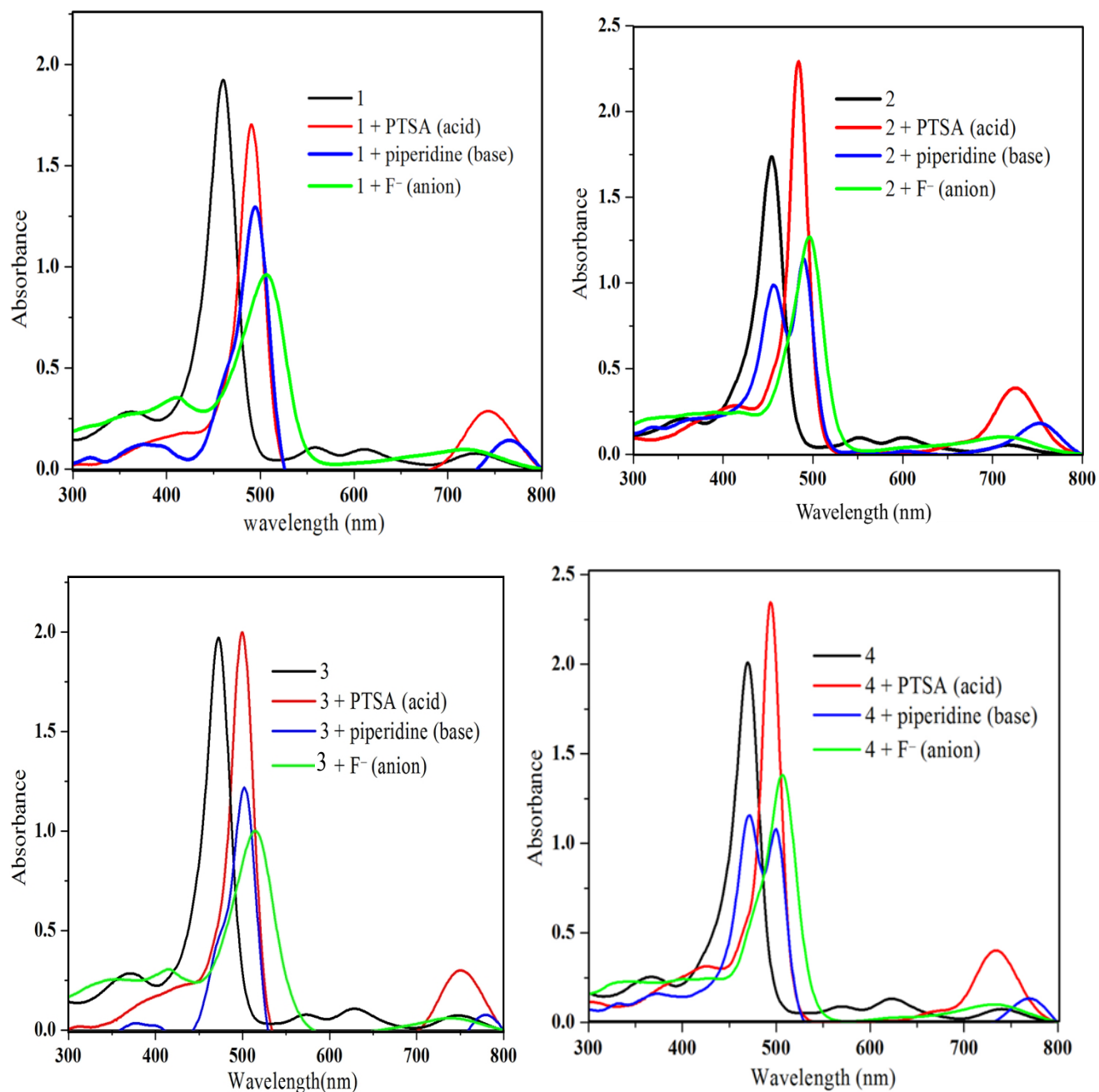
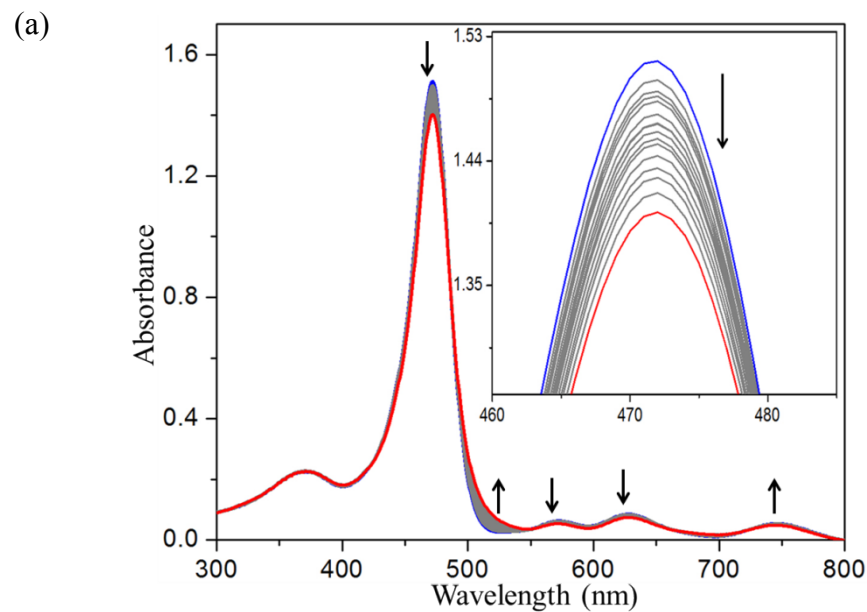


**Figure S22.** Overlayed UV-Visible Spectra of **1-4** with excess of *p*-toluenesulphonic acid (PTSA), piperidine and fluoride ions in toluene 298 K. Herein, piperidine forms 1:1 host:guest complex with **1-4** in 1,2-dichloroethane as reported in literature (Ref. P. Bhyrappa and P. Bhavana, *Chem. Phys. Lett.* 2002, **357**, 108).



(b)

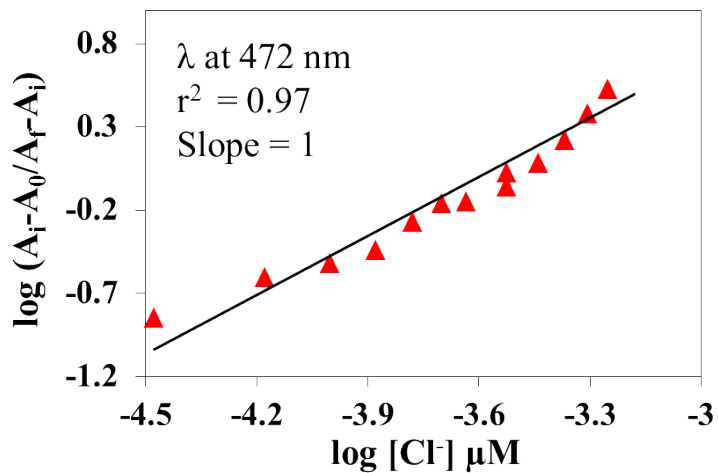


**Figure S23.** (a) UV-Vis spectral titrations of **3** with TBACl (0.008 M) in toluene at 298 K. Inset shows the absorbance changes in the Soret region; (b) Hill plot  $\log(\text{A}_i - \text{A}_0 / \text{A}_f - \text{A}_i)$  vs.  $\log [\text{Cl}^-]$  showing 1:1 stoichiometry indicated by slope 1.

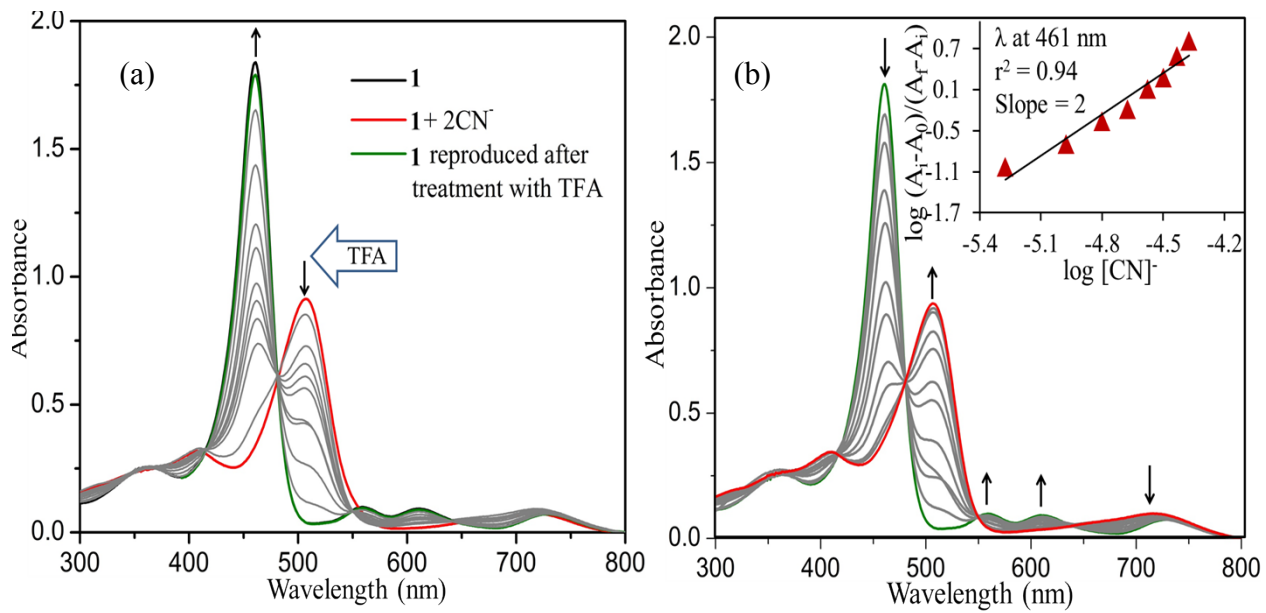


**Figure S24.** (a) Treatment of **1**• $2\text{CN}^-$  complex with aliquots of 1 mM solution TFA at 298 K. (b) Reusability test of regenerated **1** with aliquots of 8 mM solution of  $\text{CN}^-$  ions in toluene at 298 K.

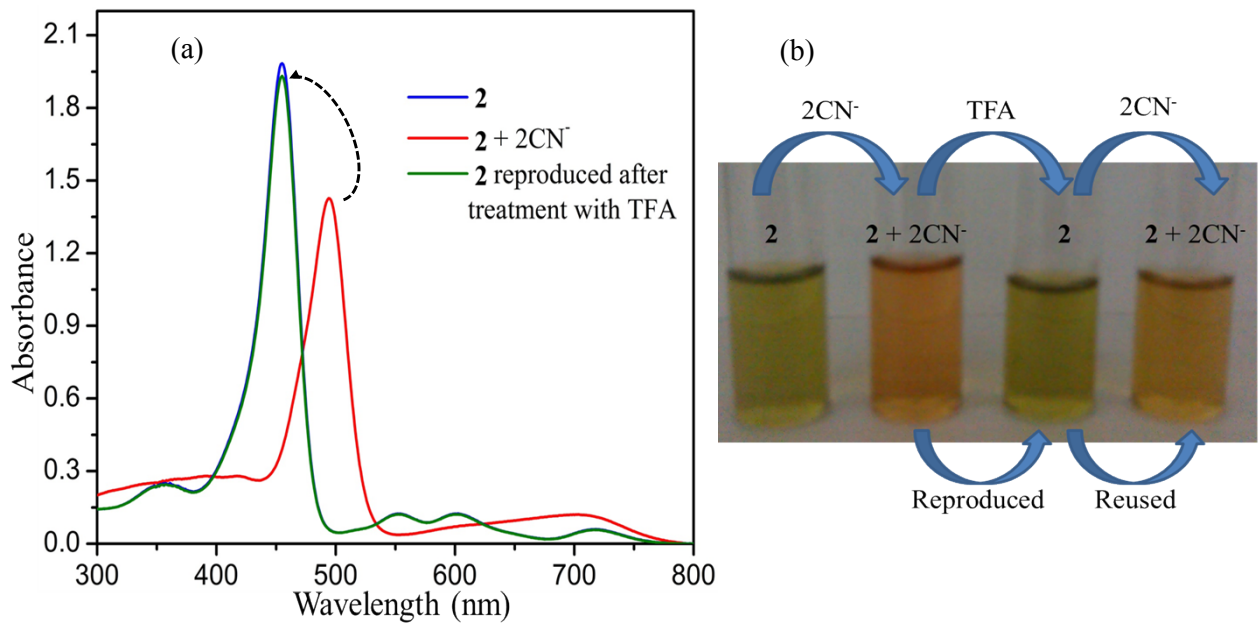


**Figure S25.** (a) Treatment of **2**• $2\text{CN}^-$  complex with sufficient amount of TFA and (b) the colorimetric response for reversibility and reusability test.

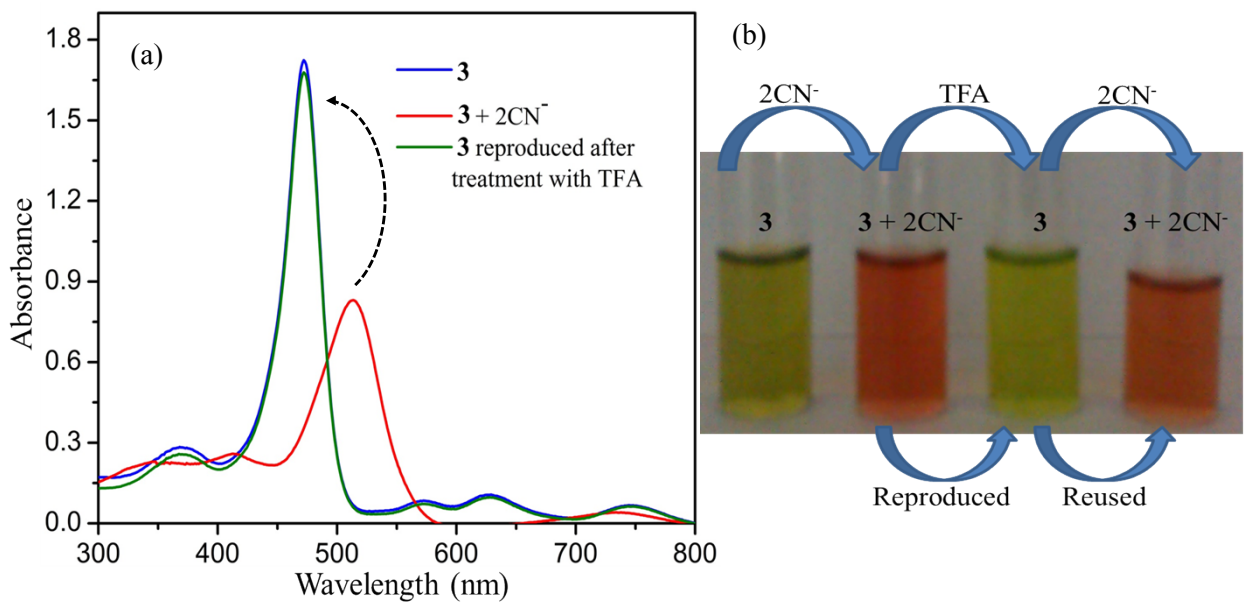


**Figure S26.** (a) Treatment of **3•2CN<sup>-</sup>** complex with sufficient amount of TFA and (b) the colorimetric response for reversibility and reusability test.

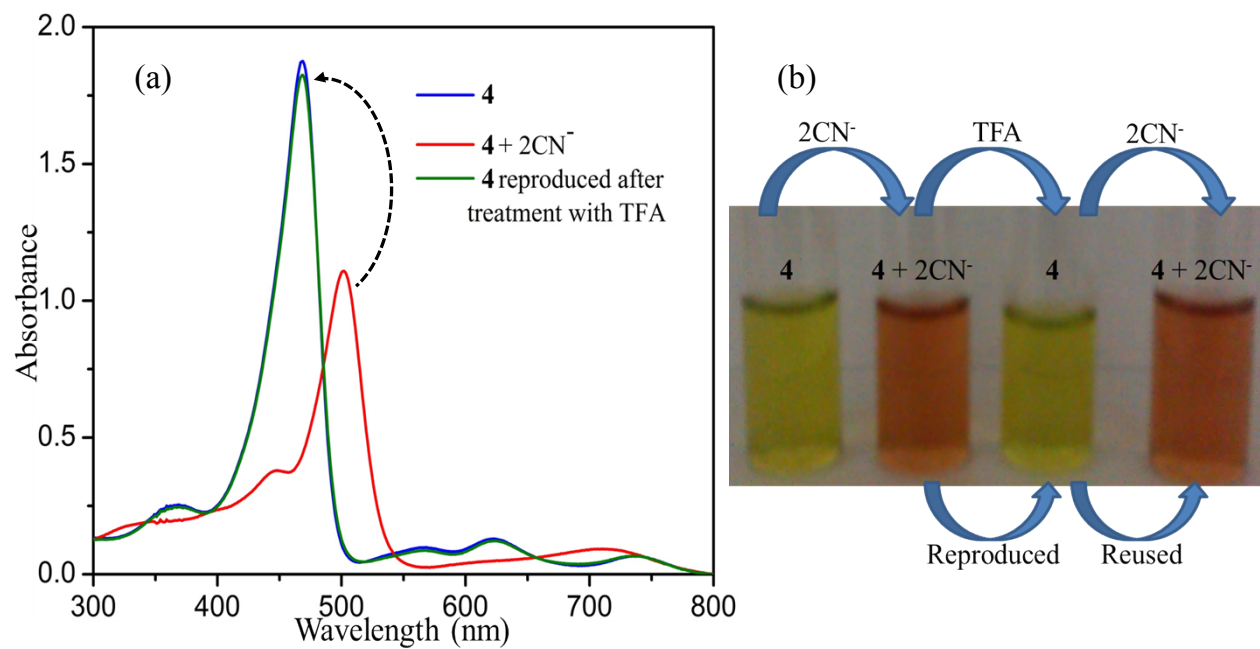


**Figure S27.** (a) Treatment of **4•2CN<sup>-</sup>** complex with sufficient amount of TFA and (b) the colorimetric response for the reversibility and reusability test.